

**INVESTIGATIONS ON POWER ALLOCATION ALGORITHMS  
IN MASSIVE MIMO**

*A Project report submitted in partial fulfilment of the requirements for  
the award of the degree of*

**BACHELOR OF TECHNOLOGY**

**IN**

**ELECTRONICS AND COMMUNICATION ENGINEERING**

*Submitted by*

N.Gayathri (318126512162)

G.Avinash (318126512136)

M.Lalitha (319126512L17)

N.Sai Srinivas (318126512159)

**Under the guidance of**

**Mr. B Chandra Mouli**

**Assistant Professor**



**DEPARTMENT OF ELECTRONICS AND COMMUNICATION  
ENGINEERING**

**ANIL NEERUKONDA INSTITUTE OF TECHNOLOGY AND SCIENCES**

**(UGC AUTONOMOUS)**

*(Permanently Affiliated to AU, Approved by AICTE and Accredited by NBA & NAAC  
with 'B+' Grade)*

Sangivalasa, bheemili mandal, visakhapatnam dist.(A.P)

2020-2021

**DEPARTMENT OF ELECTRONICS AND COMMUNICATION**

**ENGINEERING**

**ANIL NEERUKONDA INSTITUTE OF TECHNOLOGY AND SCIENCES  
(UGC AUTONOMOUS)**

*(Permanently Affiliated to AU, Approved by AICTE and Accredited by NBA &  
NAAC with 'B+' Grade)*

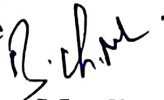
**Sangivalasa, Bheemili mandal, Visakhapatnam dist.(A.P)**



**CERTIFICATE**

This is to certify that the project report entitled “**INVESTIGATIONS ON POWER ALLOCATION ALGORITHMS IN MASSIVE MIMO**” submitted by N. Gayathri (318126512162), G. Avinash (318126512136), M. Lalitha (319126512L17), N.Sai Srinivas (318126512159), in partial fulfilment of the requirements for the award of the degree of Bachelor of Technology in Electronics & Communication Engineering of Andhra University, Visakhapatnam is a record of bonafide work carried out under my guidance and supervision.

**Project Guide**



**Mr. B Chandra Mouli**

Assistant Professor

Department of ECE

ANITS

**Assistant Professor  
Department of E.C.E.**

**Anil Neerukonda**

**Institute of Technology & Sciences  
Sangivalasa, Visakhapatnam-531 162**

**Head of the Department**

**Dr.V. Rajyalakshmi**

**Professor & HOD**

Department of ECE

ANITS

**Head of the Department  
Department of ECE**

**Anil Neerukonda Institute of Technology & Sciences  
Sangivalasa-531 162**

## **ACKNOWLEDGEMENT**

We would like to express our deep gratitude to our project guide **Mr. B. Chandra Mouli** Designation, Department of Electronics and Communication Engineering, ANITS, for his guidance with unsurpassed knowledge and immense encouragement. We are grateful to **Dr. V. Rajyalakshmi**, Head of the Department, Electronics and Communication Engineering, for providing us with the required facilities for the completion of the project work.

We are very much thankful to the **Principal and Management, ANITS, Sangivalasa**, for their encouragement and cooperation to carry out this work.

We express our thanks to all **teaching faculty** of Department of ECE, whose suggestions during reviews helped us in accomplishment of our project. We would like to thank **all non-teaching staff** of the Department of ECE, ANITS for providing great assistance in accomplishment of our project.

We would like to thank our parents, friends, and classmates for their encouragement throughout our project period. At last, but not the least, we thank everyone for supporting us directly or indirectly in completing this project successfully.

### **PROJECT STUDENTS**

**N. Gayathri (318126512162)**

**G. Avinash (318126512136)**

**M. Lalitha (319126512L17)**

**N. Sai Srinivas (318126512159)**

## ABSTRACT

Massive MIMO communication systems have recently attracted a lot of attention. The ability to increase both spectral efficiency (SE) and energy efficiency (EE) makes it one of the key technologies for the 5G cellular networks. In this work, we investigate downlink power control in massive MIMO. Due to the spatial separation between antenna arrays, power control in massive MIMO is a challenging problem. Power allocation in massive MIMO is a pivotal technique to achieve a uniform quality of service for every user throughout the network. The issue of energy and bandwidth problem are among the issues that need to be solved and developed first. It is understood that power allocation algorithms have been focused on solving these two problems. The comparison of three different power allocation algorithms, which will be among the basic power allocation algorithms, are carried out in terms of spectrum efficiency.

In addition, the use of deep learning to perform max-min and max-prod power allocation in the downlink of Massive MIMO networks. More precisely, a deep neural network is trained to learn the map between the positions of user equipment (UEs) and the optimal power allocation policies, and then used to predict the power allocation profiles for a new set of UEs' positions. The use of deep learning significantly improves the complexity-performance trade-off of power allocation, compared to traditional optimization-oriented methods. Particularly, the proposed approach does not require the computation of any statistical average, which would be instead necessary by using standard methods, and is able to guarantee near-optimal performance.

**Keywords:** Massive MIMO, Spectral efficiency, Energy efficiency, Power control, Power allocation, Neural network.

# CONTENTS

|   |      |
|---|------|
| <b>LIST OF SYMBOLS</b>                              | viii |
| <b>LIST OF FIGURES</b>                              | x    |
| <b>LIST OF TABLES</b>                               | xi   |
| <b>LIST OF ABBREVIATIONS</b>                        | xii  |
| <b>CHAPTER 1 Massive MIMO</b>                       |      |
| 1.1 MIMO  | 1    |
| 1.2 Massive MIMO                                    | 3    |
| 1.2.1 Spectral Efficiency                           | 4    |
| 1.2.2 Energy Efficiency                             | 4    |
| 1.2.3 Reliability                                   | 4    |
| 1.2.4 Increases Network Capacity                    | 5    |
| 1.2.5 Enhances Network Coverage                     | 5    |
| 1.2.6 Complements Beamforming                       | 5    |
| 1.2.7 Enables Next-Gen Technologies                 | 6    |
| 1.3 Disadvantages of Massive MIMO                   | 6    |
| 1.4 Duplexing                                       | 7    |
| 1.4.1 Frequency Division Duplexing                  | 8    |
| 1.4.2 Time Division Duplexing (TDD)                 | 9    |
| 1.5 Spatial Multiplexing and Spatial Diversity      | 10   |
| 1.6 Importance of channel in wireless communication | 12   |
| 1.6.1 Additive of White Gaussian Noise              | 13   |
| 1.6.2 Rayleigh Channel                              | 15   |

## **CHAPTER 2 SYSTEM MODEL**

|   |    |
|---|----|
| 2.1 Introduction  | 17 |
| 2.2 Multi Cell Massive MIMO system  | 19 |
| 2.2.1 Uplink Channel Estimation under Perfect Channel Knowledge               | 21 |
| 2.2.2 Uplink Channel Estimation Under Limited Channel<br>covariance knowledge | 22 |
| 2.3 Massive MIMO network  | 24 |
| 2.4 Channel Estimation  | 24 |
| 2.5 Spectral Efficiency   | 25 |
| 2.5.1 Achievable UL Spectral Efficiencies                                     | 26 |
| 2.5.2 Achievable DL Spectral Efficiencies                                     | 27 |
| 2.6 Downlink Spectral Efficiency  | 28 |
| 2.7 Precoding   | 28 |
| 2.7.1 Linear Precoding  | 29 |
| 2.7.2 Linear Precoding Algorithms   | 31 |
| 2.7.3 Precoding design  | 33 |

## **CHAPTER 3 POWER ALLOCATION IN MASSIVE MIMO**

|   |    |
|---|----|
| 3.1 Introduction                          | 35 |
| 3.1.1 Preliminaries                       | 35 |
| 3.2 Power Control with Given SINR Targets | 37 |
| 3.2.1 Single-Cell System                  | 38 |
| 3.2.2 Multi-Cell System                   | 38 |
| 3.3 Power Allocation                      | 39 |

## **CHAPTER 4 DIFFERENT TYPES OF POWER ALLOCATION**

|   |    |
|---|----|
| 4.1 Introduction                              | 42 |
| 4.2 Equal Power allocation                    | 42 |
| 4.3 Maximum-Minimum fairness Power allocation | 44 |
| 4.4 Maximum product SINR Power allocation     | 46 |

|  |    |
|--|----|
| 4.5 Deep Learning Based Power allocation | 48 |
| 4.5.1 Online Implementation              | 49 |
| 4.6 Performance Evaluation               | 50 |
| 4.6.1 Maximum Product SINR               | 50 |
| 4.6.2 Maximum-Minimum fairness           | 51 |

## **CHAPTER 5 SIMULATION RESULTS**

## **CHAPTER 6 CONCLUSIONS**

## **REFERENCES**

## **PAPER PUBLICATION DETAILS**

## LIST OF SYMBOLS

|                    |   |
|--------------------|---|
| $BS_j$             | BS in the $j$ th cell                                       |
| $BS_j^n$           | $n$ th sub-array in the $j$ th cell                         |
| $U_{jk}$           | $k$ th user in the $j$ th cell                              |
| $h_{jk}^{ln}$      | uplink channel between $U_{jk}$ and $BS_j^n$                |
| $R_{jk}^{ln}$      | channel covariance matrix                                   |
| $\phi_{jk}$        | pilot sequence  |
| $\tau_p$           | number of pilot samples per coherence interval              |
| $N_{jn}$           | additive white Gaussian noise (AWGN) at $BS_j^n$            |
| $\rho_{tr}$        | normalised pilot power per user                             |
| $\rho$             | transmitted average power                                   |
| $D_x$              | diagonal matrix with the elements of $x$ on its signal      |
| $\alpha$           | pathloss coefficient  |
| $Y$                | median channel gain   |
| $\ X\ $            | euclidean norm of the vector $x$                            |
| $\beta_{li}^j$     | average channel gain from BS $j$ to UE $i$ in cell $l$      |
| $I^M$              | $M \times M$ identity matrix                                |
| $SINR_{jk}^{dl}$   | downlink SINR of UE $j$ in cell $k$                         |
| $\gamma_{jk}^{dl}$ | downlink mean square channel estimate of UE $j$ in cell $k$ |
| $SE_{jk}^{dl}$     | downlink SE of UE $j$ in cell $k$                           |
| $\tau_d / \tau_c$  | prelog factor   |
| $V_{jk}$           | combining vector of UE $k$ in cell $j$                      |



|                   |   |
|-------------------|---|
| $\rho_{ul}$       | uplink SNR                                |
| $\rho_{dl}$       | downlink SNR                              |
| $SINR_k$          | effective SINR for the kth terminal       |
| $\overline{SINR}$ | common SINR with max-min fairness control |
| $\eta_k$          | power control coefficient                 |
| $\beta_k$         | large scale fading between k and BS       |
| $h_k$             | small scale fading between k and BS       |
| $H(Y)$            | entropy of received signal                |
| $H(N)$            | entropy of noise signal                   |
| $E\{x\}$          | expected value of the random variable x   |

## LIST OF FIGURES

| <b>Figure no</b> | <b>Title</b>  | <b>pageno</b> |
|------------------|---|---------------|
| Fig 1.1          | Basic Structure of MIMO   | 2             |
| Fig 1.2          | Massive MIMO Uplink and Downlink  | 3             |
| Fig 1.3          | FDD requires two symmetrical segments of spectrum for the uplink and downlink channels    | 9             |
| Fig 1.4          | TDD alternates the transmission and reception of station data over time                   | 10            |
| Fig 1.5          | Additive white gaussian noise   | 14            |
| Fig 1.6          | Additive Noise  | 15            |
| Fig 1.7          | Gaussian Noise  | 15            |
| Fig 2.1          | An illustration of the multi-cell DAA massive MIMO system                                 | 21            |
| Fig 2.2          | Generalized block diagram of communication systems with precoding and decoding techniques | 32            |

## LIST OF TABLES

| <b>Table no</b> | <b>Title</b>  | <b>pageno</b> |
|-----------------|---|---------------|
| Table 3.1       | Explicit formulas for the coefficients $\{a_k\}$ and $\{b_k^{k'}\}$ for a single-cell system  | 39            |
| Table 3.2       | Explicit formulas for the coefficients $\{a_{lk}\}$ , $\{b_{lk}^{l'k'}\}$ , $\{c_{lk}^{l'k'}\}$ and $\{d_{lk}^{l'k'}\}$ for a multi-cell system | 39            |
| Table 3.3       | Summary of constraints on the power control coefficients  | 40            |
| Table 4.1       | Used parameters in massive MIMO network   | 45            |

## LIST OF ABBREVIATIONS

|         |  |
|---------|--|
| MIMO    | multiple-input-multiple-output               |
| UL      | uplink                                       |
| DL      | downlink                                     |
| OFDM    | orthogonal frequency-division multiplexing   |
| SU-MIMO | single client multiple-input-multiple-output |
| MU-MIMO | multi client multiple-input-multiple-output  |
| UE      | user equipment                               |
| SE      | spectral efficiency                          |
| EE      | energy efficiency                            |
| TDD     | time-division duplexing                      |
| FDD     | frequency-division duplexing                 |
| CSI     | channel state information                    |
| LTE     | long- term- evolution                        |
| NR      | new radio                                    |
| AWGN    | additive white Gaussian noise                |
| PSD     | power spectral density                       |
| TWDP    | two-wave with diffusion power                |
| LS      | least square                                 |
| LoS     | line of sight                                |
| MMSE    | minimum mean-square error                    |
| ML      | maximum likelihood                           |
| DAA     | distributed antenna array                    |

|         |   |
|---------|---|
| EW-MMSE | element-wise minimum mean-square error  |
| M-MMSE  | multi-cell minimum mean-square error    |
| SINR    | signal-to-interference-plus-noise ratio |
| SNR     | signal-to-noise ratio                   |
| MF      | matched filtering                       |
| CB      | conjugate beamforming                   |
| MR      | maximum ratio                           |
| ZF      | zero forcing                            |
| EPA     | equal power allocation                  |

## **Chapter 1: Massive MIMO**

### **1.1 MIMO**

MIMO stands for 'Multiple Input, Multiple Output', and is a form of radio antenna that increases efficiency by increasing the number of transmitters and receivers. Perhaps more importantly, MIMO antennas can send and receive signals over the same channel, without the need to take turns, which increases capacity without sacrificing spectrum.

In today's 4G and 5G networks, base station antennas are typically fitted with around 12 antenna ports that broadcast information in every direction at once. Which means that current transceivers have to take turns if they want to transmit and receive data on the same frequency, or the data has to be moved to another frequency to avoid hold-ups, and this causes congestion.

In radio, multiple-input and multiple-output, or MIMO, is a method for multiplying the capacity of a radio link using multiple transmission and receiving antennas to exploit multipath propagation. MIMO has become an essential element of wireless communication standards including IEEE 802.11n (Wi-Fi 4), IEEE 802.11ac (Wi-Fi 5), HSPA+ (3G), WiMAX, and Long-Term Evolution (LTE). More recently, MIMO has been applied to power-line communication for three-wire installations as part of the ITU G.hn standard and of the HomePlug AV2 specification.

At one time, in wireless the term "MIMO" referred to the use of multiple antennas at the transmitter and the receiver. In modern usage, "MIMO" specifically refers to a practical technique for sending and receiving more than one data signal simultaneously over the same radio channel by exploiting multipath propagation. Although the "multipath" phenomenon may be interesting, it is the use of orthogonal frequency-division multiplexing (OFDM) to encode the channels that is responsible for the increase in data capacity. MIMO is fundamentally different from smart antenna techniques developed to enhance the performance of a single data signal, such as beamforming and diversity.

MIMO systems are an indispensable piece of current wireless systems, and lately they have been utilized broadly to accomplish high spectral effectiveness and energy productivity. Prior to the presentation of MIMO, single-input-single-output systems were for the most part utilized, which had exceptionally low throughput and couldn't support countless clients with high dependability. To oblige this massive client interest, different new MIMO innovation like single-client MIMO (SU-MIMO), multi-client MIMO (MU-MIMO) and organization MIMO were created. Be that as it may, these new innovations are additionally insufficient to oblige the always expanding requests. The wireless clients have expanded dramatically over the most recent couple of years, and these clients create trillions of information that should be taken care of productively with greater dependability.

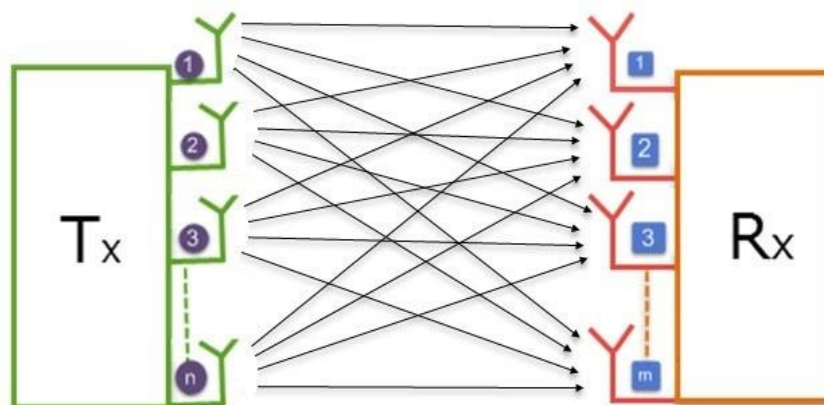


**Figure 1.1** Basic Structure of MIMO

## 1.2 Massive MIMO

Massive MIMO is the most dazzling innovation for 5G and past the wireless access period. Massive MIMO is the headway of contemporary MIMO systems utilized in current wireless organizations, which groups together hundreds and even large number of antennas at the base station and serves many clients at the same time. The additional antennas that massive MIMO uses will help center energy into a more modest area of room to give better spectral proficiency and throughput.

**Definition 1.1:** (Massive MIMO), Massive MIMO is a type of wireless communications technology in which base stations are equipped with a very large number of antenna elements to improve spectral and energy efficiency. Massive MIMO systems typically have tens, hundreds, or even thousands of antennas in a single antenna array.

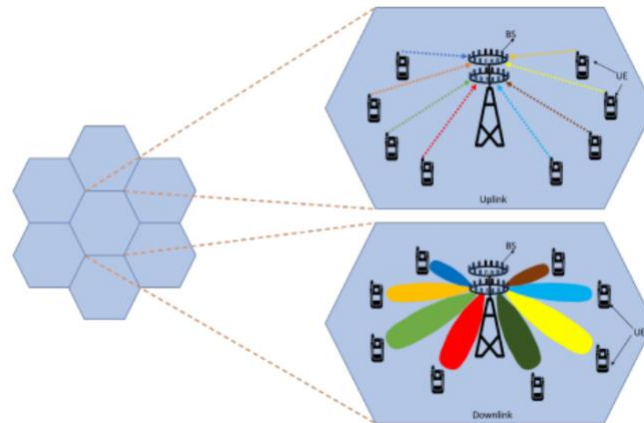


**Figure 1.2** Massive MIMO Uplink and Downlink

- It uses SDMA to achieve a multiplexing gain by serving multiple UEs on the same time-frequency resources.
- It has more BS antennas than UEs per cell to achieve efficient interference suppression. If the anticipated number of UEs grows in a cell, the BS should be upgraded so that the number of antennas increases proportionally.
- It operates in TDD mode to limit the CSI acquisition overhead, due to the multiple antennas, and to not rely on parameterizable channel models.

## 1.2 Advantages of Massive MIMO

Massive MIMO fundamentally expands the capabilities of MU-MIMO through the inclusion of a higher number of antennas to bring drastic improvements in network performance. Hence, it has become one of the technological underpinnings of modern wireless cellular networks to include the 4G standard, LTE and LTE Advanced technologies, and 5G technologies. Placing a large number of antennas allow a particular access point to focus the transmission and reception of electromagnetic signals to specific regions or targeted areas, thus improving throughput, capacity, and



efficiency. Note that a Massive MIMO system also coordinates the operation of these antennas through machine learning and algorithm.

### **1.2.1 Spectral Efficiency**

Massive MIMO systems achieve a high spectral efficiency by exploiting a large antenna array to originate more multiplexing gain. Consequently, each user equipment has an individual down-beam which leads to offering spectral efficiencies ten times higher than that in the conventional MIMO technology.

### **1.2.2 Energy Efficiency**

In massive MIMO systems, the gain of transmitted signals is increased to the position of candidate users by pointing the beam of the antenna array into a small region. Consequently, the massive MIMO systems radiate less power and are more energy-efficient systems. Moreover, the transmit power is significantly reduced when the number of transmit antennas is increased. By dint of the huge number of antennas in massive MIMO systems, a BS can make several beams at the same time and directly pointing them to a particular user or more. Then, the resources can be used repeatedly in the same specific area. Thus, the throughput could be increased without increasing the transmit power by increasing the number of transmit antennas. Massive MIMO systems have the ability to reduce the transmitted power 1000 times below conventional MIMO and to maximize the data rates at the same time.

### **1.2.3 Reliability**

A large number of antennas in massive MIMO systems advances high diversity gain, which increases the link reliability and elasticity against fading.

### **1.2.4 Increases Network Capacity**

Massive MIMO increases the capacity of a particular wireless communication network in two ways. First, it enables the deployment of higher frequencies, such as in the case of Sub-6 5G specification. Second, by employing multi-user MIMO, a cellular base station with Massive MIMO capability can send and receive multiple data streams simultaneously from different users using the same frequency resources.

Note that network capacity is determined by the number or amount of total data a particular network can serve to its end-users, as well as by the maximum number of end-users that can be served based on an expected service level.

### **1.2.5 Enhances Network Coverage**

Another advantage of Massive MIMO is that it provides high spectral efficiency through the coordination of multiple antennas using simple processing and without intensive power consumption. When used in a 5G cellular network technology, it allows 10 times more spectral and network efficiency compared to fourth-generation networks. Furthermore, when applied in 4G technology, it improves the deep coverage of fourth-generation networks.

Because next-generation cellular network technologies use electromagnetic radiation with higher frequencies or more specifically, frequencies within the upper limits of radio waves and the range of microwaves, the signals they generate travel a short distance. Hence, enhancing network coverage is critical in modern and future cellular technologies.

### **1.2.6 Complements Beamforming**

Beamforming technology works by focusing a signal toward a specific direction, rather than broadcasting in all directions, thus resulting in more direct communication between a transmitter and a receiver, more stable and reliable connectivity, and faster data transmission. As a signal processing technique and traffic-signalling system, this technology depends on advanced antenna technologies on both access points and end-user devices.

The large number of antennas in a Massive MIMO system enables three-dimensional beamforming in which a single beam of signal-bearing electromagnetic radiation travels through vertical and horizontal directions. The process increases data transmission rates further while reaching people in elevated areas such as buildings and those in moving vehicles

### **1.2.7 Enables Next-Gen Technologies**

Massive MIMO is an essential component of 5G technology. For example, in Sub-6 5G specification, it allows the utilization of frequencies within the sub-6 GHz range. Moreover, in mmWave 5G specification, this technology increases frequency reach to expand network coverage, optimizes the propagation of signal-bearing electromagnetic radiation, and allows true multi-user wireless communication within a defined area.

### **1.3 Disadvantages of Massive MIMO**

One of the biggest disadvantages of Massive MIMO is the cost associated with its implementation and deployment. The systems are several times more extensive than traditional base station units and antenna technologies. Furthermore, the design of multiple antenna systems for cellular networks is more complex and requires more effort and time during assembly and installation.

Furthermore, using frequency division duplex or FDD results in feedback overhead. This phenomenon transpires when a receiver sends out feedback signals to a transmitter. Increasing the antenna elements results in a further increase in the overhead. Hence, time-division duplex or TDD is more suitable for Massive MIMO implementation.

The placement of multiple antennas in a defined area within a base station means placing hardware components in a smaller space. An entire massive multiple-input and multiple-output system needs advanced components that are capable of

delivering their intended level of performance despite their smaller size than their larger counterparts. Remember that Massive MIMO is not simply about placing and using a large number of antennas. The entire technology also works using artificial intelligence and machine learning to complement frequency management, signal processing techniques, and data transmission. Doing so requires complex processing algorithms that further add to the cost and complexity of designing, implementing, and deploying an entire system.

#### **1.4 Duplexing**

A duplex communication system is a point-to-point system composed of two or more connected parties or devices that can communicate with one another in both directions. Duplex systems are employed in many communications networks, either to allow for simultaneous communication in both directions between two connected parties or to provide a reverse path for the monitoring and remote adjustment of equipment in the field.

It takes two forms:

1. Half duplex
2. Full duplex

In half duplex, the two communicating parties take turns transmitting over a shared channel. Two-way radios work this way. As one-party talks, the other listens. Speaking parties often say “Over” to indicate that they’re finished and it’s time for the other party to speak. In networking, a single cable is shared as the two computers communicating take turns sending and receiving data.

Full duplex refers to simultaneous two-way communications. The two communicating stations can send and receive at the same time. Landline telephones and cell phones work this way. Some forms of networking permit simultaneous transmit and receive operations to occur. This is the more desirable form of duplexing, but it is more complex and expensive than half duplexing.

There are two basic forms of full duplexing:

1. Frequency division duplex (FDD)
2. Time division duplex (TDD)

### 1.4.1 Frequency Division Duplexing

FDD requires two separate communications channels. In networking, there are two cables. Full-duplex Ethernet uses two twisted pairs inside the CAT5 cable for simultaneous send and receive operations. Wireless systems need two separate frequency bands or channels (Fig 1.2). A sufficient amount of guard band separates the two bands so the transmitter and receiver don't interfere with one another. Good filtering or duplexers and possibly shielding are a must to ensure the transmitter does not desensitize the adjacent receiver.

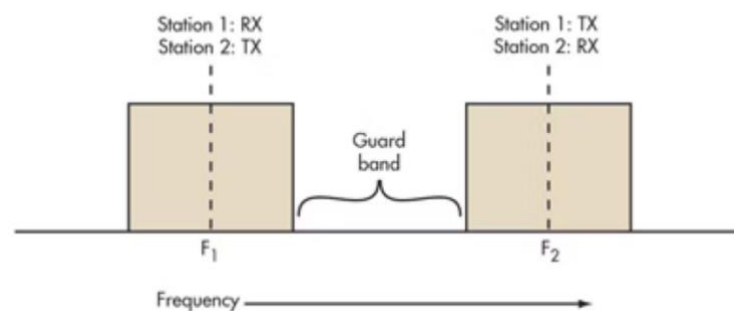


**Figure 1.3** FDD requires two symmetrical segments of spectrum for the uplink and downlink channels

In a cell phone with a transmitter and receiver operating simultaneously within such close proximity, the receiver must filter out as much of the transmitter signal as possible. The greater the spectrum separation, the more effective the filters.

FDD uses lots of frequency spectrum, though, generally at least twice the spectrum needed by TDD. In addition, there must be adequate spectrum separation between the transmit and receive channels. These so-called guard bands aren't useable, so they're wasteful. Given the scarcity and expense of spectrum, these are real disadvantages.

However, FDD is very widely used in cellular telephone systems, such as the widely used GSM system. In some systems the 25-MHz band from 869 to 894 MHz is used as the downlink (DL) spectrum from the cell site tower to the handset, and the 25-MHz band from 824 to 849 MHz is used as the uplink (UL) spectrum from the handset to cell site.

Another disadvantage with FDD is the difficulty of using special antenna techniques like multiple-input multiple-output (MIMO) and beamforming. These technologies are a core part of the new Long-Term Evolution (LTE) 4G cell phone strategies for increasing data rates. It is difficult to make antenna bandwidths broad enough to cover both sets of spectrum. More complex dynamic tuning circuitry is required.

#### 1.4.2 Time Division Duplexing (TDD)

TDD uses a single frequency band for both transmit and receive. Then it shares that band by assigning alternating time slots to transmit and receive operations (Fig 1.3). The information to be transmitted—whether it's voice, video, or computer data—is in serial binary format. Each time slot may be 1 byte long or could be a frame of multiple bytes.

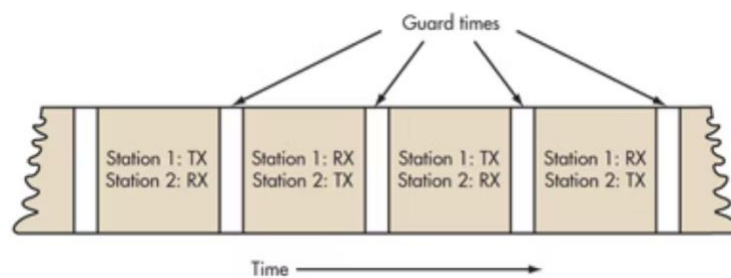


**Figure 1.4** TDD alternates the transmission and reception of station data over time.

In some TDD systems, the alternating time slots are of the same duration or have equal DL and UL times. However, the system doesn't have to be 50/50 symmetrical. The system can be asymmetrical as required. For instance, in Internet

access, download times are usually much longer than upload times so more or fewer frame time slots are assigned as needed. The real advantage of TDD is that it only needs a single channel of frequency spectrum. Furthermore, no spectrum-wasteful guard bands or channel separations are needed. The downside is that successful implementation of TDD needs a very precise timing and synchronization system at both the transmitter and receiver to make sure time slots don't overlap or otherwise interfere with one another.

### **1.5 Spatial Multiplexing and Spatial Diversity**

Spatial multiplexing and spatial diversity are two radio communication techniques used in modern antenna systems in 4G LTE and 5G NR networks. Both these techniques play essential but separate roles in the MIMO (Multiple Input Multiple Output) antenna systems.

**Definition 1.2:** (Spatial Diversity). Spatial diversity is a technique in MIMO that reduces signal fading by sending multiple copies of the same radio signal through multiple antennas. Spatial diversity improves radio signal link quality by employing multiple antennas at the transmitter or receiver to communicate numerous copies of the same signal. That allows the antennas to overcome the negative impact of multipath fading by using the copies of the signal to reconstruct it.

Diversity is not a new concept in mobile communications and has been used for years to address the negative impact of signal fading. When a radio signal (e.g., a mobile signal) travels from the cellular base station to the receiver of a mobile phone, it can take many routes depending on the obstructions in its way. Obstructions can be things like buildings, trees, poles, mountains etc. When the signal encounters any obstructions, it can get scattered and become weak or “fade” by the time it reaches the receiver. Diversity in radio communications is the ability of an antenna system to create redundant network resources for the signal to minimise the overall impact of signal fading. In plain English, it means creating additional copies of the signal so that bits and pieces of the scattered signal can be picked up to reconstruct the signal. At a

theoretical level, at least three types of diversity solutions are available, including frequency, time, and space diversity. Frequency diversity requires multiple frequency channels, each communicating a version or copy of the same signal. Time diversity does the same thing but uses different time-slots instead so that different copies of the signal are communicated at different time intervals. But the diversity type employed by MIMO antenna systems is space diversity, also known as spatial diversity. In MIMO systems, spatial diversity is achieved by multiple antennas at the transmitter and the receiver that communicate (transmit or receive) a different version of the same signal. These versions are essentially a replica of the original signal. If used at the receiver end, the receiver can collect all the different versions of the signal to reconstruct it to overcome the negative impact of signal fading. In 4G LTE and 5G NR networks, spatial diversity is a critical part of MIMO systems that use multiple antennas at the transmitter and the receiver.

**Definition 1.3** (Spatial Multiplexing). spatial multiplexing is a technique in MIMO that boosts data rates by sending the data payload in separate streams through spatially separated antennas. Spatial multiplexing improves data rates by allowing the overall data payload to be communicated to a user device in the form of multiple data streams that carry small portions of the overall information. The data streams can be targeted at a single user device or multiple user devices.

Spatial multiplexing or Space Division Multiplexing (SDM) is a multiplexing technique employed by MIMO antenna systems. It is an essential feature of MIMO and is the primary reason for introducing MIMO in 4G LTE and 5G NR networks. In spatial multiplexing, a transmitter or receiver can use several antennas separated in space by their angular direction. These antennas can send and receive multiple data streams using the same frequency and time resources and act as individual channels to communicate the information (e.g. a WhatsApp message) between the transmitter and receiver. The multiple data streams within a MIMO system can target a single user device or multiple user devices for simultaneous communication. When the data payload is sent towards a user device in the form of multiple concurrent streams, the data rate for the user device



goes up. 5G NR networks use an enhanced version of MIMO, called Massive MIMO which consists of tens or even hundreds of antenna elements within a single antenna panel. Due to the sheer volume of antenna elements and the multi-user support capability, Massive MIMO can simultaneously offer higher data rates to several user devices.

MIMO systems in 4G LTE and 5G NR networks use both spatial multiplexing and spatial diversity to improve data rates whilst improving signal quality. In MIMO, spatial diversity is a technique that provides the ability to overcome the negative impact of multipath signal fading by communicating separate versions or copies of the same signal through multiple antennas. On the other hand, spatial multiplexing is a technique that improves the achievable data rates for end-users by transmitting and receiving multiple streams of data through various spatially-separated antennas.

### **1.6 Importance of channel in wireless communication**

Communicating data or an information signal from transmitter or receiver to receiver or transmitter requires some form of path way or medium called CHANNEL. Channel plays an important role in wireless communication since it can degrade the information signal by adding multipath fading and Doppler effects (if channel is mobile). Correct knowledge of channel is a fundamental prerequisite for the design of a wireless communication system. A communication channel either to a physical transmission medium such as wire, or through a local connection over a multiplexed medium such as a radio channel.

A channel is used to convey an information signal from one of several senders to one of several receivers. A channel has a certain capacity  $E$ , for transmitting information often measured by its bandwidth in Hz or its data rate in bits per second. Bandwidth is a limited resource used by different organizations due to which widespread use of wireless networks is limited. The wireless channel is susceptible to a variety of transmission impediments, path loss, interference and blockage. These factors restrict the range and the reliability of the wireless transmission to the extent to which these factors

affect the transmission depends upon the environmental conditions and the mobility of the transmitter and the receiver.

### 1.6.1 Additive white Gaussian Noise

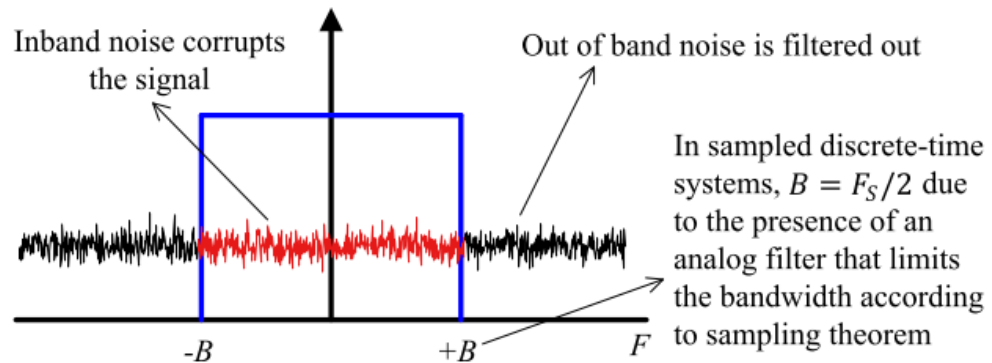


**Figure 1.5** Additive white gaussian noise

The performance of a digital communication system is quantified by the probability of bit detection errors in the presence of thermal noise. In the context of wireless communications, the main source of thermal noise is addition of random signals arising from the vibration of atoms in the receiver electronics.

The term additive white Gaussian noise (AWGN) originates due to the following reasons Additive: The noise is additive, Le., the received signal is equal to the transmitted signal plus noise. This gives the most widely used equality in communication systems.

$$r(t)=s(t)+w(t) \quad (1)$$

which is shown in Figure below. Moreover, this noise is statistically independent of the signal Remember that the above equation is highly simplified due to neglecting every single imperfection a Tx signal encounters, except the noise itself.

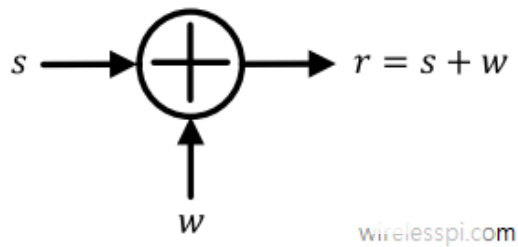


**Figure 1.6** Additive Noise

**White:** Just like the white colour which is composed of all frequencies in the visible spectrum, white noise refers to the idea that it has uniform power across the whole frequency band. As a consequence, the Power Spectral Density (PSD) of white noise is constant for all frequencies ranging from  $-\infty$  to  $+\infty$ .

**Gaussian:** The probability distribution of the noise samples is Gaussian with a zero mean,  $e$ , in time domain, the samples can acquire both positive and negative values and in addition, the values close to zero have a higher chance of occurrence while the values far away from zero are less likely to appear. This is shown in Figure below. As a result, the time domain average of large number of noise samples is equal to zero.

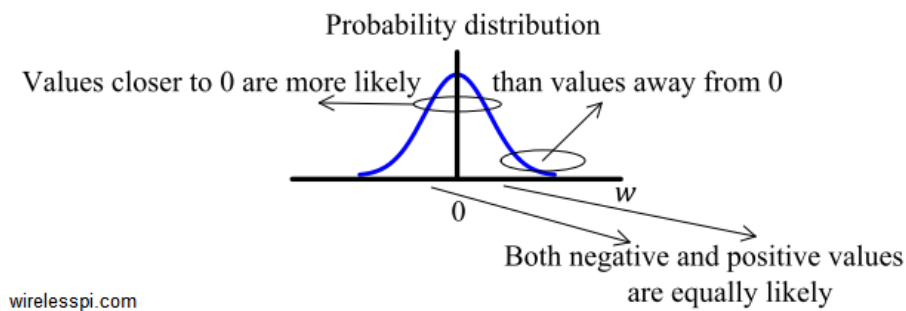


**Figure 1.7** Gaussian Noise

In reality, the ideal flat spectrum from  $-\infty$  to  $+\infty$  is true for frequencies of interest in wireless communications (a few kHz to hundreds of GHz) but not for higher frequencies. Nevertheless, every wireless communication system involves filtering that removes most of the noise energy outside the spectral band occupied by our desired signal. Consequently, after filtering, it is not possible to distinguish whether the spectrum was ideally flat or partially flat outside the band of interest. To help in

mathematical analysis of the underlying waveforms resulting in closed-form expressions — a holy grail of communication theory — it can be assumed to be flat before filtering. For a discrete signal with sampling rate  $FS$ , the sampling theorem dictates that the bandwidth of a signal is constrained by a lowpass filter within the range  $\pm FS/2$  to avoid aliasing. For the purpose of calculations, this filter is an ideal lowpass filter with

$$H(F) = \begin{cases} 1, & -\frac{FS}{2} < F < +\frac{FS}{2} \\ 0, & \text{elsewhere} \end{cases} \quad (2)$$

The resulting in-band power is shown in red in the figure below, while the rest is filtered out.

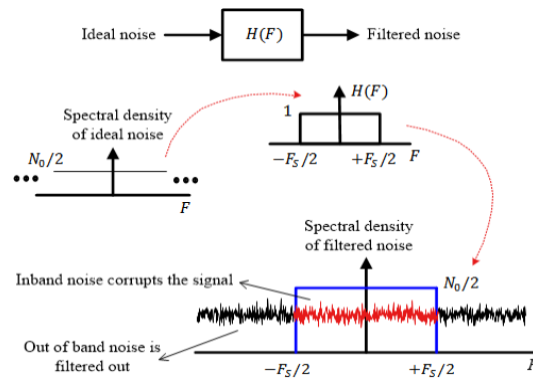


**Figure 1.8** Additive white gaussian noise

### 1.6.2 Rayleigh Channel

Rayleigh fading is a statistical model for the effect of a propagation environment on a radio signal, such as that used by wireless devices. Rayleigh fading models assume that the magnitude of a signal that has passed through such a transmission medium (also called a communication channel) will vary randomly, or fade, according to a Rayleigh distribution, the radial component of the sum of two uncorrelated Gaussian random variables.

Rayleigh fading is viewed as a reasonable model for tropospheric and ionospheric signal propagation as well as the effect of heavily built-up urban environments on radio signals. Rayleigh fading is most applicable when there is no

dominant propagation along a line of sight between the transmitter and receiver. If there is a dominant line of sight, Rician fading may be more applicable. Rayleigh fading is a special case of two-wave with diffuse power (TWDP) fading.

Rayleigh fading is a reasonable model when there are many objects in the environment that scatter the radio signal before it arrives at the receiver. The central limit theorem holds that, if there is sufficiently much scatter, the channel impulse response will be well-modelled as a Gaussian process irrespective of the distribution of the individual components. If there is no dominant component to the scatter, then such a process will have zero mean and phase evenly distributed between 0 and  $2\pi$  radians. The envelope of the channel response will therefore be Rayleigh distributed. Calling this random variable, it will have a probability density function:

$$p_R(r) = \frac{2r}{\Omega} e^{-r^2/\Omega}, \quad r \geq 0 \quad (3)$$

Where  $\Omega = E(R^2)$ .

Often, the gain and phase elements of a channel's distortion are conveniently represented as a complex number. In this case, Rayleigh fading is exhibited by the assumption that the real and imaginary parts of the response are modelled by independent and identically distributed zero-mean Gaussian processes so that the amplitude of the response is the sum of two such processes.

Rayleigh channel model: The Rayleigh fading environment is described by the many multipath components, each having relatively similar signal magnitude, and uniformly distributed phase, that means there is no line of sight (LoS) path between transmitter and receiver. The channel in which the signal takes various paths to reach the receiver after getting reflected from various objects in the environment. The signal received at the receiver is the sum of the reflected signal and the main signal. The signal in the environment gets diffracted or reflected from the objects like trees, buildings, moving vehicles etc and imposes a problem when the envelope of the individual signal is added up.

## CHAPTER 2: SYSTEM MODEL

### 2.1 Introduction:

Channel estimation is crucial for massive multiple-input multiple-output (MIMO) systems to scale up multi-user (MU) MIMO, providing great improvement in spectral and energy efficiency. The expected massive MIMO improvements assume that accurate channel estimations are available at both the receiver and transmitter for detection and precoding, respectively. Additionally, the reuse of frequencies and pilot reference sequences in cellular communication systems causes interferences in channel estimation, degrading its performance. Since both the time-frequency resources allocated for pilot transmission and the channel coherence time are limited, the number of possible orthogonal pilot sequences is also limited, and as a consequence, the pilot sequences have to be reused in neighbour cells of cellular systems. Therefore, channel estimates obtained in a given cell get contaminated by the pilots transmitted by the users in other cells. This coherent interference is known in the literature as pilot contamination, i.e., the channel estimate at the base station in one cell becomes contaminated by the pilots of the users from other cells. The contamination not only reduces the quality of the channel estimates, i.e., increases the MSE, but also makes the channel estimates statistically dependent, even though the true channels are statistically independent. Moreover, pilot contamination does not disappear with the addition of more antennas.

Massive MIMO systems operating in TDD assume channel reciprocity between uplink and downlink in order to minimize pilot overhead, transmitting pilot reference signals only in the uplink. In this scenario, pilot overhead cost is proportional to the number of terminals and improved estimation quality can be achieved due to the large number of antennas. Base stations estimate channels usually based on least squares (LS) or minimum mean square error (MMSE) methods. Besides, inter and intra-cell large-scale fading coefficients are assumed to be perfectly known when applying the MMSE method in the great majority of works.

In a real-world network deployment, although changing slowly, the large-scale fading coefficients must be estimated and updated from time to time. Additionally, the estimation error of the large-scale fading coefficients impacts significantly on the performance of uplink data decoding and downlink transmission (e.g., precoding and beamforming). Approaches on how to estimate the large-scale fading coefficients are presented in the following pieces of work.

The most commonly used analytical massive MIMO channel is the spatially frequency non-selective (flat) fading channel model. Flat fading channels are also known as amplitude varying channels and narrowband channels as the signal's bandwidth is narrow compared to channel's bandwidth. In this narrowband channel model, the channel gain between any pair of transmit-receive antennas is determined as a complex Gaussian random variable. This model relies on two assumptions: (i) the antenna elements in the transmitter and receiver being spatially well separated once the more widely spaced (in wavelengths) the antenna elements, the smaller the spatial channel correlation, and (ii) the presence of a large number of temporally but narrowly separated multipaths (common in a rich-scattering environment), whose combined gain, by the central-limit theorem, can be approximated by a Gaussian random variable.

Flat fading channels present a channel response that exhibits flat gain and linear phase over a bandwidth (coherence bandwidth) that is greater than the signal's bandwidth. Therefore, all frequency components of the signal will experience the same magnitude of fading, resulting in a scalar channel response. The gain applied to the signal varies over time according to a fading distribution. In this work, we consider that the gain applied to the signal passing through this channel will vary randomly, according to a Rayleigh distribution. We additionally assume that the antenna spacing is sufficiently large so that the antennas are uncorrelated.

The channel estimation and pilot contamination problems associated with uplink training in flat Rayleigh fading channels and understand its impact on the operation of multi-cell MU massive MIMO TDD cellular systems. We propose and evaluate an efficient and practical channel estimator that does not require previous

knowledge of inter/intra-cell large-scale fading coefficients (i.e., interference) and noise power. Differently from, we employ the maximum likelihood (ML) method to find an estimator for the interference plus noise power term in the MMSE channel estimator. We show that this estimator is not only unbiased but also achieves the Crámer-Rao lower bound. We replace this estimator back into the MMSE estimator and prove that the performance of the new channel estimator asymptotically approaches that of the MMSE estimator.

## 2.2 Multi cell Massive MIMO system:

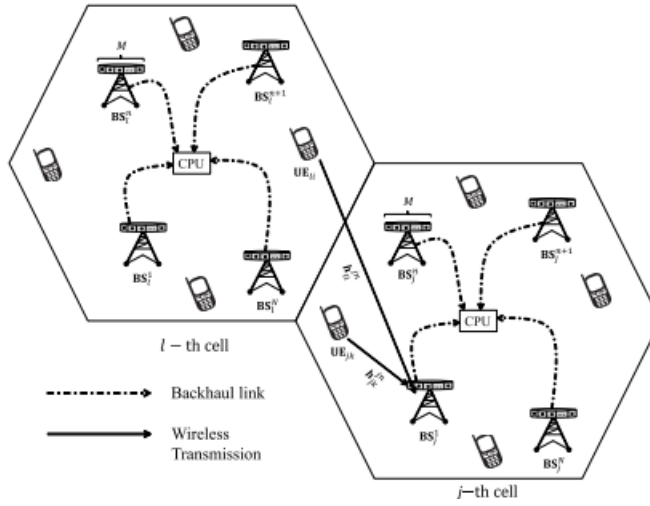


**Figure 2.1** An illustration of the multi-cell DAA massive MIMO system.

we consider a multi-cell multi-user massive MIMO network, as illustrated in Fig(2.1) The network consists of  $L$  cells with  $K$  single-antenna users in each cell<sup>1</sup>. Notably, each cell has  $N$  DAAs deployed at arbitrary locations, where each sub-array is equipped with  $M$  antenna elements. As such, there are  $M_{\text{tot}} = M \times N$  antenna elements in each cell.

Each sub-array in a cell is connected to a CPU through backhaul links<sup>2</sup>. We highlight that no coordination is required between different cells in the system and CPU in each cell only requires local information via a backhaul links that can be implemented using cloud-RAN techniques. Furthermore, we assume that there is perfect synchronization in the system. We denote the BS in the  $j$ -th cell by  $BS_j$ , where



$j \in \{1, \dots, L\}$ . The  $n$ -th antenna sub-array in the  $j$ -th cell is represented by  $\text{BS}_j^n$  where  $n \in \{1, \dots, N\}$ . Furthermore, we represent the  $k$ -th user in the  $j$ -th cell by  $U_{jk}$ , where  $k \in \{1, \dots, K\}$ . We represent the uplink channel between  $U_{jk}$  and  $\text{BS}_j^n$  by  $h_{jk}^{ln}$ , where  $l \in \{1, \dots, L\}$ . Additionally, we assume that the channels follow a correlated Rayleigh fading distribution, i.e.,  $h_{jk}^{ln} \sim \text{CN}(0, R_{jk}^{ln})$ , where  $R_{jk}^{ln}$  is the channel covariance matrix, which encapsulates various channel impairments such as average path-loss and spatial correlation. We clarify that the path loss between a user and all antenna elements of a DAA is considered constant. However, due to the physical separation between various DAAs the path losses between a users and different DAAs in a cell are not constant. As such, the existing power control algorithm cannot be applied to the system model considered in our work.

The system model considered is a generalized model as compared to since it is capable of describing various antenna array deployments. For example, we note that the cell free massive MIMO is a special case of our considered system model when  $L = 1$ ,  $M = 1$ , and  $N = M_{\text{tot}}$ . Moreover, co-located massive MIMO is another special case of our considered system model when  $M = M_{\text{tot}}$  and  $N = 1$ .

We assume the network operates in the time division duplex (TDD) mode. Accordingly, the uplink and downlink channels are assumed to be the same and reciprocal within one channel coherence interval. Consequently, the BS utilizes the uplink channel estimates for downlink precoding based on the assumption of channel reciprocity. In the beginning of each channel coherence interval, the users in each cell transmit their pilot sequences to the same-cell BS, which then performs channel estimation. The channel estimation is followed by the downlink data transmission where each BS sends data to the same-cell users.

### 2.2.1 Uplink Channel Estimation Under Perfect Channel Knowledge

At the beginning of each channel coherence interval, all users send their pre-assigned pilot sequences to the same cell BS for the purpose of channel estimation. We denote the pilot sequence assigned to  $U_{jk}$  by  $\phi_{jk}$ , where  $\|\phi_{jk}\|$ ,  $j \in \{1, \dots, L\}$ , and  $k \in \{1, \dots, K\}$ . We assume that each pilot sequence is of length  $\tau_p$ . We highlight that we need to estimate the channels between a user and all the same-cell DAAs in the system. Differently, in co-located massive MIMO, the channel estimation is typically performed between a user and a single same-cell BS. Furthermore, we assume that each user within the same cell is assigned an orthogonal pilot sequence, i.e.,  $\tau_p = K$ . The same set of pilot sequences are reused in each cell across the entire network. Consequently, the uplink pilot transmission received at the  $n^{\text{th}}$  sub-array of  $BS_j$ , i.e.,  $BS_j^n$ , is given as

$$\mathbf{Y}^{jn} = \sum_{l=1}^L \sum_{i=1}^K \mathbf{h}_{li}^{jn} \phi_{li}^H + \frac{1}{\sqrt{\rho_{\text{tr}}}} \mathbf{N}_j^n, \quad (1)$$

where  $\mathbf{N}_j^n \in \mathbb{C}^{M \times \tau}$  represents the additive white Gaussian noise (AWGN) at  $BS_j^n$ , and  $\rho_{\text{tr}}$  is the normalized pilot power per user. Afterwards, the sub-array  $BS_j^n$  correlates (1) with the known pilot sequence to obtain

$$\mathbf{y}_{jk}^{jn} = \left( \sum_{l=1}^L \sum_{i=1}^K \mathbf{h}_{li}^{jn} \phi_{li}^H + \frac{1}{\sqrt{\rho_{\text{tr}}}} \mathbf{N}_j^n \right) \phi_{jk}. \quad (2)$$

We denote the correlation between pilot sequences assigned to  $U_{li}$  and  $U_{jk}$  as  $\rho_{jk}^{li} = \Phi_{li}^H \Phi_{jk}$ . Based on this definition, we re-express (2) as

$$\mathbf{y}_{jk}^{jn} = \mathbf{h}_{jk}^{jn} + \sum_{\substack{l=1 \\ (l,i) \neq (j,k)}}^L \sum_{i=1}^K \rho_{li}^{jk} \mathbf{h}_{li}^{jn} + \frac{1}{\sqrt{\rho_{\text{tr}}}} \mathbf{N}_j^n \phi_{jk}. \quad (3)$$

From (3), we obtain the MMSE uplink channel estimate, i.e.,  $\hat{\mathbf{h}}_{jk}^{jn}$  of the channel  $\mathbf{h}_{jk}^{jn}$  as

$$\hat{\mathbf{h}}_{jk}^{jn} = \mathbf{W}_{jk}^n \mathbf{y}_{jk}^{jn}, \quad (4)$$

where

$$\mathbf{W}_{jk}^n = \mathbf{R}_{jk}^{jn} (\mathbf{Q}_{jk}^n)^{-1}, \quad (5)$$

$$\mathbf{R}_{jk}^{jn} = \mathbb{E} \left[ \mathbf{h}_{jk}^{jn} (\mathbf{h}_{jk}^{jn})^H \right], \quad (6)$$

and

$$\begin{aligned} \mathbf{Q}_{jk}^n &= \mathbb{E} \left[ \mathbf{y}_{jk}^{jn} (\mathbf{y}_{jk}^{jn})^H \right] \\ &= \sum_{l=1}^L \sum_{i=1}^K \left| \rho_{li}^{jk} \right|^2 \mathbf{R}_{lk}^{jn} + \frac{1}{\rho_{tr}} \mathbf{I}_M. \end{aligned} \quad (7)$$

Under the assumption of full statistical channel knowledge, the covariance matrices  $\mathbf{R}_{jk}^{jn}$  are known to the BSs. As such, BS<sub>j</sub><sup>n</sup> can obtain the matrix  $\mathbf{Q}_{jk}^n$  by using (7). Afterwards, utilizing (5) together with (3), BS<sub>j</sub><sup>n</sup> obtain the channel uplink channel estimates using (4). We highlight that the assumption of perfect channel covariance knowledge is commonly used in massive MIMO literature. Additionally, the change in the channel covariance information occurs at a slow rate. As such, the channel statistics remains largely unchanged over several channel coherence intervals. Furthermore, several methods exist in literature to estimate the change in the channel covariance information with small overhead.

### 2.2.2 Uplink Channel Estimation Under Limited Channel Covariance Knowledge:

In this subsection, we discuss a more practical scenario where BSs only have limited knowledge of the channel covariance. Specifically, we assume that BSs do not have full knowledge of the channel covariance matrix  $\mathbf{R}_{jk}^{jn}$ . Furthermore, BSs only have knowledge about the diagonal elements of the channel covariance matrices. Under these assumptions, we obtain the element-wise EW-MMSE uplink channel estimate of the  $z$ -th element of  $\mathbf{h}_{jk}^{jn}$ , where  $z \in \{1, \dots, M\}$ , as

We highlight that the diagonal elements of the channel covariance matrices are easy to estimate and require only a few additional resources. Consequently, the EW-MMSE channel estimate for  $\mathbf{h}_{jk}^{\text{in}}$  is obtained as

$$\left[\widehat{\mathbf{h}}_{jk}^{\text{in}}\right]_z = \frac{\left[\mathbf{R}_{jk}^{\text{in}}\right]_z}{\sum_{l=1}^L \sum_{i=1}^K \left|\rho_{li}^{\text{in}}\right|^2 \left[\mathbf{R}_{li}^{\text{in}}\right]_z + \frac{1}{\rho_{\text{tr}}}} \left[\mathbf{y}_{jk}^{\text{in}}\right]_z. \quad (8)$$

We highlight that the diagonal elements of the channel covariance matrices are easy to estimate and require only a few additional resources. Consequently, the EW-MMSE channel estimate for  $\mathbf{h}_{jk}^{\text{in}}$  is obtained as

$$\widehat{\mathbf{h}}_{jk}^{\text{in}} = \widehat{\mathbf{W}}_{jk}^{\text{in}} \mathbf{y}_{jk}^{\text{in}}, \quad (9)$$

where

$$\widehat{\mathbf{W}}_{jk}^{\text{in}} = \mathbf{D}_{jk}^{\text{in}} (\mathbf{\Lambda}_{jk}^{\text{in}})^{-1}. \quad (10)$$

We highlight that  $\mathbf{D}_{jk}^{\text{in}}$  and  $\mathbf{\Lambda}_{jk}^{\text{in}}$  are  $M \times M$  diagonal matrices. We define  $\mathbf{D}_{jk}^{\text{in}}$  as

$$\mathbf{D}_{jk}^{\text{in}} = \begin{bmatrix} \left[\mathbf{R}_{jk}^{\text{in}}\right]_1 & 0 & 0 & 0 \\ 0 & \left[\mathbf{R}_{jk}^{\text{in}}\right]_2 & 0 & 0 \\ 0 & 0 & \dots & 0 \\ 0 & 0 & 0 & \left[\mathbf{R}_{jk}^{\text{in}}\right]_M \end{bmatrix} \quad (11)$$

and  $\mathbf{\Lambda}_{jk}^{\text{in}}$  as

$$\begin{bmatrix} \sum_{l,i} \left|\rho_{li}^{\text{in}}\right|^2 \left[\mathbf{R}_{li}^{\text{in}}\right]_1 + \frac{1}{\rho_{\text{tr}}} & 0 & & 0 \\ 0 & \dots & & 0 \\ 0 & 0 & \sum_{l,i} \left|\rho_{li}^{\text{in}}\right|^2 \left[\mathbf{R}_{li}^{\text{in}}\right]_M + \frac{1}{\rho_{\text{tr}}} & \end{bmatrix}. \quad (12)$$

Afterwards, utilizing (10) together with (3),  $\text{BS}_j^{\text{n}}$  obtains the channel uplink channel estimates according to (9), under the assumption of imperfect channel knowledge at BSs.

### 2.3 Massive MIMO network

We consider the DL of a Massive MIMO network with  $L$  cells, each comprising a BS with  $M$  antennas and  $K$  UEs. We denote by  $\mathbf{h}_{i^l}^j \in \mathbb{C}^M$  the channel between UE  $i$  in cell  $l$  and BS  $j$  and assume that

$$\mathbf{h}_{i^l}^j \sim \mathcal{N}_{\mathbb{C}}(\mathbf{0}_M, \mathbf{R}_{i^l}^j) \quad (1)$$

where  $\mathbf{R}_{i^l}^j \in \mathbb{C}^{M \times M}$  is the spatial correlation matrix, known at the BS. The normalized trace  $\beta_{i^l}^j = 1/M \text{tr}(\mathbf{R}_{i^l}^j)$  accounts for the average channel gain from an antenna at BS  $j$  to UE  $i$  in cell  $l$  and is modelled as (in dB)

$$\beta_{i^l}^j = \Upsilon - 10\alpha \log_{10}\left(\frac{d_{i^l}^j}{1\text{km}}\right) \text{ dB} \quad (2)$$

where  $\Upsilon = -148$  dB determines the median channel gain at a reference distance of 1 km, and  $\alpha = 3.76$  is the pathloss coefficient. Also,  $d_{i^l}^j$  is the distance of UE  $i$  in cell  $l$  from BS  $j$ , given by  $d_{i^l}^j = \|\mathbf{x}_{i^l}^j\|$  with  $\mathbf{x}_{i^l}^j \in \mathbb{R}^2$  being the UE location in the Euclidean space. Note that shadowing should also be considered in (2). However, this is usually modelled by a log-normal distribution, resulting into a channel model that is not spatially consistent. In other words, two UEs at almost the same location would not experience the same channel. To overcome this issue, one should resort to channel models based on ray tracing or recorded measurements.

### 2.4 Channel Estimation

Pilot-based channel training is utilized to estimate the channel vectors at BS $_j$ . We assume that the BS and UEs are perfectly synchronized and operate according to a time division duplex (TDD) protocol wherein the DL data transmission phase is preceded in the UL by a training phase for channel estimation. There are  $\tau_p = K$  pilots (i.e., pilot reuse factor of 1) and UE  $i$  in each cell uses the same pilot. Using a total UL pilot power of  $\rho_{\text{tr}}$  per UE and standard MMSE estimation techniques, BS  $j$  obtains the estimate of  $\mathbf{h}_{i^l}^j$  as

$$\hat{\mathbf{h}}_{li}^j = \mathbf{R}_{li}^j \mathbf{Q}_{li}^{-1} \left( \sum_{l'=1}^L \mathbf{h}_{l'i}^j + \frac{1}{\tau_p} \frac{\sigma^2}{\rho} \mathbf{n}_{li} \right) \sim \mathcal{N}_{\mathbb{C}} \left( \mathbf{0}, \Phi_{li}^j \right) \quad (3)$$

where  $\mathbf{n}_{li} \sim \mathcal{N}_{\mathbb{C}}(0, \mathbf{I}_M)$  is noise,  $\mathbf{Q}_{li} = \sum_{l'=1}^L \mathbf{R}_{l'i}^j + 1/\rho_{\text{tr}} \mathbf{I}_M$ , and  $\Phi_{jli} = \mathbf{R}_{li}^j \mathbf{Q}_{li}^{-1} \mathbf{R}_{li}^j$ . The estimation error  $\mathbf{h}_{li}^j = \mathbf{h}_{li}^j - \hat{\mathbf{h}}_{li}^j \sim \mathcal{N}_{\mathbb{C}}(0, \mathbf{R}_{li}^j - \Phi_{li}^j)$  is independent of  $\hat{\mathbf{h}}_{li}^j$ .

## 2.5 Spectral Efficiency

**Definition:** The SE of an encoding/decoding scheme is the average number of bits of information, per complex-valued sample, that it can reliably transmit over the channel under consideration.

From this definition, it is clear that the SE is a deterministic number that can be measured in bit per complex-valued sample. Since there are  $B$  samples per second, an equivalent unit of the SE is bit per second per Hertz, often written in short-form as bit/s/Hz. For fading channels, which change over time, the SE can be viewed as the average number of bit/s/Hz over the fading realizations, as will be defined below. In this monograph, we often consider the SE of a channel between a UE and a BS, which for simplicity we refer to as the ‘‘SE of the UE’’. A related metric is the information rate [bit/s], which is defined as the product of the SE and the bandwidth  $B$ . In addition, we commonly consider the sum SE of the channels from all UEs in a cell to the respective BS, which is measured in bit/s/Hz/cell.

SE of a cell can be increased by using more transmit power, deploying multiple BS antennas, or serving multiple UEs per cell. All these approaches inevitably increase the PC of the network, either directly (by increasing the transmit power) or indirectly (by using more hardware), and therefore may potentially reduce the Energy Efficiency (EE).

In a broad sense, EE refers to how much energy it takes to achieve a certain amount of work. This general definition applies to all fields of science, from physics to economics, and wireless communication is no exception. Unlike many fields wherein

the definition of “work” is straightforward, in a cellular network it is not easy to define what exactly one unit of “work” is. The network provides connectivity over a certain area and it transports bits to and from UEs. Users pay not only for the delivered number of bits but also for the possibility to use the network anywhere at any time. Moreover, grading the performance of a cellular network is more challenging than it first appears, because the performance can be measured in a variety of different ways and each such performance measure affects the EE metric differently. Among the different ways to define the EE of a cellular network, one of the most popular definitions takes inspiration from the definition of SE, that is, “the SE of a wireless communication system is the number of bits that can be reliably transmitted per complex-valued sample”. By replacing “SE” with “EE” and “complex-valued sample” with “unit of energy”, the following definition is obtained.

### 2.5.1 Achievable UL Spectral Efficiencies:

The channel estimates enable each BS to semi-coherently detect the data signals from its UEs. In particular, we assume that BS  $j$  applies a linear receive combining vector  $\mathbf{g}_{jk} \in \mathbb{C}^M$  to the received signal, as  $\mathbf{g}_{jk}^H \mathbf{y}_j$ , to amplify the signal from its  $k$ th UE and reject interference from other UEs in the spatial domain. We want to derive the ergodic achievable SE for any UE, where codewords span over both the Rayleigh fading and random locations of the interfering UEs—specific UE distributions are considered. For notational convenience, we assume that  $\beta = B/K$  is an integer that we refer to as the pilot reuse factor. The cells in  $L$  are divided into  $\beta \geq 1$  disjoint subsets such that the same  $K$  pilot sequences are used within a set, while different pilots are used in different sets. We refer to this as non-universal pilot reuse. The following theorem shows how the SE depends on the receive combining, for Gaussian codebooks where  $\mathbf{x}_{jk} \sim \mathcal{CN}(0,1)$

**Theorem 1.** In the UL, an ergodic achievable SE of an arbitrary UE  $k$  in cell  $j$  is

$$\zeta^{(ul)} \left(1 - \frac{B}{S}\right) \mathbb{E}_{\{Z\}} \{ \log_2(1 + \text{SINR}_{jk}^{(ul)}) \} \quad [\text{bit/s/Hz}] \quad (1)$$

where the effective signal-to-interference-and-noise ratio (SINR),  $\text{SINR}_{jk}^{(ul)}$  is given by

$$\text{SINR}_{jk}^{(\text{ul})} = \frac{p_{jk} |\mathbb{E}_{\{\mathbf{h}\}} \{\mathbf{g}_{jk}^H \mathbf{h}_{jjk}\}|^2}{\sum_{l \in \mathcal{L}} \sum_{m=1}^K p_{lm} \mathbb{E}_{\{\mathbf{h}\}} \{|\mathbf{g}_{jk}^H \mathbf{h}_{jlm}|^2\} - p_{jk} |\mathbb{E}_{\{\mathbf{h}\}} \{\mathbf{g}_{jk}^H \mathbf{h}_{jjk}\}|^2 + \sigma^2 \mathbb{E}_{\{\mathbf{h}\}} \{\|\mathbf{g}_{jk}\|^2\}}$$

The expectations  $\mathbb{E}_{\{z\}}\{\cdot\}$  and  $\mathbb{E}_{\{\mathbf{h}\}}\{\cdot\}$  are with respect to UE positions and channel realizations, respectively.

### 2.5.2 Achievable DL Spectral Efficiencies:

The channel estimates are also used for linear precoding in the DL, where the M channel inputs are utilized to make each data signal add up semi-coherently at its desired UE and to suppress the interference caused to other UEs.  $\mathbf{w}_{jk} \in \mathbb{C}^M$  is the precoding vector associated with UE k in cell j. We express these precoding vectors as

$$\mathbf{w}_{jk} = \sqrt{\frac{q_{jk}}{\mathbb{E}_{\{\mathbf{h}\}} \{\|\check{\mathbf{g}}_{jk}\|^2\}}} \check{\mathbf{g}}_{jk}^*$$

where the average transmit power  $q_{jk} \geq 0$  is a function of the UE positions, but not the instantaneous channel realizations. The vector  $\check{\mathbf{g}}_{jk} \in \mathbb{C}^M$  defines the spatial directivity of the transmission and is based on the acquired CSI; the normalization with the average squared norm  $\mathbb{E}_{\{\mathbf{h}\}} \{\|\check{\mathbf{g}}_{jk}\|^2\}$  gives the analytic tractability that enables the following results.

**Theorem 2.** In the DL, an ergodic achievable SE of an arbitrary UE k in cell j is

$$\zeta^{(\text{dl})} \left(1 - \frac{B}{S}\right) \mathbb{E}_{\{Z\}} \{\log_2(1 + \text{SINR}_{jk}^{(\text{dl})})\} \quad [\text{bit/s/Hz}] \quad (2)$$

with the effective SINR,  $\text{SINR}_{jk}^{(\text{dl})}$ , given by

$$\frac{q_{jk} \frac{|\mathbb{E}_{\{\mathbf{h}\}} \{\check{\mathbf{g}}_{jk}^H \mathbf{h}_{jjk}\}|^2}{\mathbb{E}_{\{\mathbf{h}\}} \{\|\check{\mathbf{g}}_{jk}\|^2\}}}{\sum_{l \in \mathcal{L}} \sum_{m=1}^K q_{lm} \frac{\mathbb{E}_{\{\mathbf{h}\}} \{|\check{\mathbf{g}}_{lm}^H \mathbf{h}_{ljk}|^2\}}{\mathbb{E}_{\{\mathbf{h}\}} \{\|\check{\mathbf{g}}_{lm}\|^2\}} - q_{jk} \frac{|\mathbb{E}_{\{\mathbf{h}\}} \{\check{\mathbf{g}}_{jk}^H \mathbf{h}_{jjk}\}|^2}{\mathbb{E}_{\{\mathbf{h}\}} \{\|\check{\mathbf{g}}_{jk}\|^2\}} + \sigma^2}$$



## 2.6 Downlink Spectral Efficiency:

The BS in cell  $l$  transmits the DL signal  $x_l = \sum_{k=1}^K w_{lk} \zeta_{lk}$  where  $\zeta_{lk} \sim \mathcal{N}_C(0, \rho_{lk})$  is the DL data signal intended for UE  $k$  in cell  $l$ , assigned to a precoding vector  $w_{lk} \in \mathbb{C}^M$  that determines the spatial directivity of the transmission and satisfies  $\|w_{lk}\|^2 = 1$  so that  $\rho_{lk}$  represents the transmit power. An achievable DL SE can be computed in Massive MIMO by using the following hardening bound .

**Theorem 3.** The DL ergodic channel capacity of UE  $k$  in cell  $j$  is lower bounded by

$$SE_{jk}^{\text{dl}} = \frac{\tau_d}{\tau_c} \log_2 (1 + \gamma_{jk}^{\text{dl}}) \quad [\text{bit/s/Hz}] \quad (3)$$

with

$$\gamma_{jk}^{\text{dl}} = \frac{\rho_{jk} |\mathbb{E}\{\mathbf{w}_{jk}^H \mathbf{h}_{jk}^j\}|^2}{\sum_{l=1}^L \sum_{i=1}^K \rho_{li} \mathbb{E}\{|\mathbf{w}_{li}^H \mathbf{h}_{jk}^l|^2\} - \rho_{jk} |\mathbb{E}\{\mathbf{w}_{jk}^H \mathbf{h}_{jk}^j\}|^2 + \sigma^2} \quad (4)$$

where the expectations are computed with respect to the channel realizations. The pre-log factor  $\frac{\tau_d}{\tau_c}$  accounts for the fraction of samples per coherence block used for DL data.

Notice that the above lower bound is achieved when the UE treats the mean of its precoded channel as the true one. This is a reasonable assumption for channels that exhibit channel hardening, but a certain loss occurs for channels with little or no hardening.

## 2.7 Precoding

**Definition:** Precoding is the transmitter signal processing needed to affect the received signal's maximization to specific receivers and antennas while reducing the interference to all other receivers and receiving antennas.

Precoding is a conception of beam-forming where the multi-antenna systems support the multi-stream transmission. Precoding performs an imperious technique in massive MIMO systems where it plays a crucial role to reduce the effects of interference and path-loss, and increases the throughput. In massive MIMO systems, the BS can estimate the CSI thanks to the UL pilot signals which are sent from the received terminals. The received CSI at the BS is imperfect and uncontrollable as a result of several environmental obstacles on the wireless channel. Though the BS does not have a perfect CSI, nevertheless the DL performance of the BS broadly depends on the estimated CSI. The massive MIMO's BS exploits the precoding techniques and the estimated CSI to mitigate the interference and increase spectral efficiency.

The precoding techniques give a tremendous benefits to massive MIMO systems. Unfortunately, these benefits are coming with a high computational complexity which is directly proportional to the number of antennas. Therefore, a low complexity precoder is imperative to exploit in massive MIMO systems.

### 2.7.1 Linear Precoding

The below Fig 2.2 depicts the generalized block diagrams of communication systems with precoding and decoding techniques. The  $\mathbf{P}$  is a feedforward matrix of linear precoding, the  $\mathbf{B}$  is a feedback matrix of linear precoding, the  $\mathbf{K}$  is a feedforward matrix of linear decoding, and the  $\mathbf{C}$  is a feedback matrix of non-linear precoding. These matrices specify the required precoding technique from a linear/non-linear or hybrid technique. For instance, when  $\mathbf{B} = 0$  the generalized precoding technique acts as the linear precoding technique. The Modulo arithmetic is used to adjust the average power.

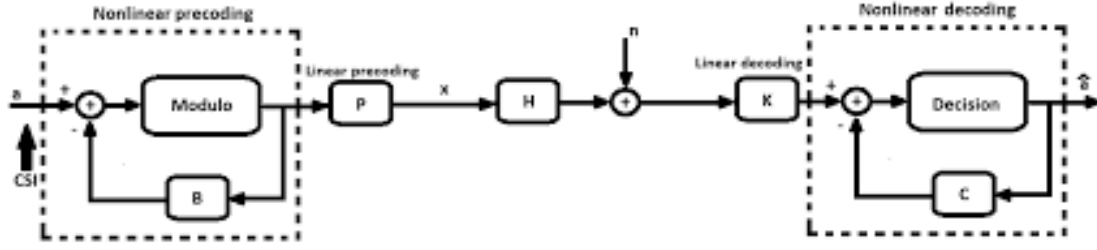


**Figure 2.2** Generalized block diagram of communication systems with precoding and decoding techniques.

Thus the transmitted signal for the  $N$  users in the DL transmission, where  $M > N$ , can be expressed as:

$$\mathbf{x} = \sqrt{\rho} \mathbf{P} \mathbf{a}, \quad \mathbf{x} \in \mathbb{C}^{M \times 1} \quad (1)$$

where  $\mathbf{P}$  is a  $M \times N$  linear precoding matrix,  $\mathbf{a}$  is a  $N \times 1$  transmitted vector before precoding process, and  $\sqrt{\rho}$  is the transmitted average power. The precoding matrix  $\mathbf{P}$  is related to  $\mathbf{H}$ . In the TDD mode, the DL channel is the transpose of the  $\mathbf{H}$ , and the  $N \times 1$  vector at  $N$ -received terminals becomes

$$\begin{aligned} \mathbf{y} &= \mathbf{H}^T \mathbf{x} + \mathbf{n}, \\ &= \sqrt{\rho} \mathbf{H}^T \mathbf{P} \mathbf{a} + \mathbf{n}, \quad \mathbf{y} \in \mathbb{C}^{N \times 1} \end{aligned} \quad (2)$$

In general, the  $\mathbf{P}$  matrix of basic precoding techniques contains a matrix inversion operation which leads to high computational complexity, especially, if  $N$  is not greater enough than  $M$ . According to the manner of dealing with the matrix inversion process, the linear precoding technique can be classified into basic linear precoding, linear precoder based on the matrix inversion approximation, linear precoder based on fixed-point iterations, and linear precoder based on matrix-decomposition.

### 2.7.2 Linear Precoding Algorithms

The basic linear precoder mainly depends on multiplying the transmitted signal  $\mathbf{a}$  with the precoding matrix  $\mathbf{P}$ . The basic linear precoder has  $O(N^3)$  computational complexity which is comparable to the exact matrix inversion complexity.

#### A) Maximum Ratio (MR) Algorithm

The MR aims to maximize the gain of signal into a specific receive terminal. It is the counterpart of the matched filtering (MF) and conjugate beamforming (CB). The MR precoding matrix formula is

$$\mathbf{P}_{\text{MRT}} = \sqrt{\beta} (\mathbf{H}^*) \quad (1)$$

where  $\beta$  is a scaling power factor and  $\mathbf{H}^*$ 's the complex conjugate of  $\mathbf{H}$  matrix. Thus, the received signal becomes

$$\mathbf{y}_{\text{MRT}} = \sqrt{\beta} \sqrt{\rho} \mathbf{H}^T \mathbf{H}^* \mathbf{a} + \mathbf{n}, \quad \mathbf{y} \in \mathbb{C}^{N \times 1} \quad (2)$$

The MR algorithm achieves the sum capacity of a massive MIMO system when the number of  $M$  is much larger than  $N$ , and  $M$  grows to infinity ( $M \gg N$  and  $M \rightarrow \infty$ ).

In general, the MR algorithm performance is close to optimal when the inter-user interference (IUI) is trivial compared to the noise (noise-limited systems). In the MR algorithm, when the values of  $M$  and  $N$  are comparable, the system experiences a strong IUI. Thus, the throughput of each user becomes low which degenerates the massive MIMO concept. Another amazing feature of the MR algorithm is that each antenna in the BS can perform its signal processing locally. That allows a decentralized construction for the large number of antennas and leads to a great flexible system.

#### B) Zero-Forcing (ZF) Algorithm

The ZF algorithm is a common algorithm of fundamental precoding techniques. It is the counterpart of the channel inversion. A ZF algorithm mitigates the interference caused of other users by pointing the signal beam into the intended user whereas nulling the other directions where other users are located. This nulling is performed by multiplying the user data with the following ZF precoding matrix.

$$\mathbf{P}_{\text{ZF}} = \sqrt{\beta} \mathbf{H}^* (\mathbf{G}^{-1}) \quad (1)$$

where  $\mathbf{G} = \mathbf{H}^T \mathbf{H}^*$  is a Gram matrix whose diagonal components indicate power imbalance through the channel, and non-diagonal components indicate the mutual correlations among the channels. While the number of transmit antennas grows to infinity in massive MIMO systems,  $\mathbf{G}$  goes to become an identity matrix and the matrix inversion computations can be simplified. The received signal of the ZF algorithm can be expressed as

$$\mathbf{y}_{\text{ZF}} = \sqrt{\beta} \sqrt{\rho} \mathbf{H}^T \mathbf{H}^* (\mathbf{G}^{-1}) \mathbf{a} + \mathbf{n}, \quad \mathbf{y} \in \mathbb{C}^{N \times 1} \quad (2)$$

The ZF algorithm performance is close to optimal when the noise is trivial compared to the IUI. The ZF algorithm is considered to be practical when neglecting the AWGN in the massive MIMO channel model, while the massive MIMO precoding algorithm becomes much simpler to implement. Unfortunately, the noise is not negligible in a real situation and utilization of the ZF algorithm in massive MIMO systems may not give an optimal solution. The ZF algorithm may achieve accurate results at high signal-to-noise ratio (SNR).

### C) Minimum Mean Square Error (MMSE) Algorithm

The MMSE algorithm exploits the benefits of the MR and ZF algorithms and achieves a balance between them. Therefore, it has an acceptable performance in moderate noise and interference systems. The MMSE algorithm is the counterpart of the regularized ZF (RZF), signal-to-leakage and-interference ratio (SLNR), eigenvalue-based beamforming, and transmit Wiener filtering. The MMSE algorithm is created by using the mean square error method in the signal to minimize the error filtering between the transmitted symbols from the BS and the received terminal.

The MMSE precoding matrix formula is

$$\mathbf{P}_{\text{MMSE}} = \sqrt{\beta} \mathbf{H}^* (\mathbf{G} + \mathbf{V} + \lambda \mathbf{I}_N)^{-1} \quad (1)$$

where  $\lambda$  is a positive regularizing factor which depends on the system dimensions, the noise variance, and uncertainty of channel at the transmitter. The matrix  $\mathbf{V}$  is a  $N \times N$  deterministic Hermitian non-negative definite matrix. When  $\mathbf{V} = \mathbf{0}$ , a balance occurs between increasing the channel gain toward intended received terminals (at a large value of  $\lambda$ ) and eliminating the IUI (at a small value of  $\lambda$ ). The MMSE algorithm performs as the ZF algorithm at  $\lambda \rightarrow 0$ , and as the MF algorithm at  $\lambda \rightarrow \infty$ . The received signal of the MMSE algorithm is

$$\mathbf{y}_{\text{MMSE}} = \sqrt{\beta} \sqrt{\rho} \mathbf{H}^T \mathbf{H}^* (\mathbf{G} + \mathbf{V} + \lambda \mathbf{I}_N)^{-1} \mathbf{a} + \mathbf{n}$$

However, the computation of the ZF and MMSE precoding matrix comprises the inversion of a very large-dimension matrix, particularly for large values of  $M$  and  $N$ . Therefore, it is quite important to offer a method to diminish the complexity of the basic precoding algorithms.

### 2.7.3 Precoding design

Unlike in the UL, finding the optimal precoders is a challenging task since the DL SE in (5) depends on the precoding vectors  $\{\mathbf{w}_{li}\}$  of all UEs in the entire network. Motivated by the UL-DL duality, a common heuristic approach is to select  $\mathbf{w}_{jk}$  as

$$\mathbf{w}_{jk} = \frac{\mathbf{v}_{jk}}{\|\mathbf{v}_{jk}\|} \quad (1)$$

where  $\mathbf{v}_{jk}$  denotes the combining vector used to detect the UL signal transmitted by UE  $k$  in cell  $j$ . In this work, we assume that  $\mathbf{v}_{jk}$  is designed according to MR combining

$$\mathbf{v}_{jk}^{\text{MR}} = \hat{\mathbf{h}}_{jk}^j \quad (2)$$

and M-MMSE combining

$$\mathbf{v}_{jk}^{M\text{-MMSE}} = \left( \sum_{l=1}^L \sum_{i=1}^K \hat{\mathbf{h}}_{li}^j (\hat{\mathbf{h}}_{li}^j)^H + \mathbf{Z}_j \right)^{-1} \hat{\mathbf{h}}_{jk}^j \quad (3)$$

where

$$\mathbf{Z}_j = \sum_{l=1}^L \sum_{i=1}^K (\mathbf{R}_{li}^j - \Phi_{li}^j) + \frac{\sigma_{\text{ul}}^2}{\rho_{\text{ul}}} \mathbf{I}_M \quad (4)$$

This choice is motivated by the fact that M-MMSE is optimal but has high computational complexity. On the other hand, MR is suboptimal (not only for finite values of  $M$  but also as  $M \rightarrow \infty$ ) but has the lowest complexity among the receive combining schemes.

## CHAPTER 3: POWER ALLOCATION IN MASSIVE MIMO

### 3.1 Introduction

Effective and computationally tractable power control is one of the unique new features of Massive MIMO. Among other things, power control handles near-far effects, and it enables uniformly good service throughout the cell. Massive MIMO power control occurs on a long time scale because effective SINRs depend only on large-scale fading coefficients. We develop power control schemes to meet given performance targets both in single-cell and multi-cell systems and both for the uplink and the downlink, with max-min (egalitarian) SINR fairness as a particularly important special case.

Power allocation in massive MIMO is a pivotal technique to achieve uniform quality of service for every user throughout the network. We highlight that power allocation is performed to utilize the available power in an efficient manner. During the uplink transmission phase, power control methods for power allocation can be applied to mitigate the near far effects. Furthermore, during the downlink transmission, power control can be applied to ensure that every user in the network enjoys a uniform quality of service. Power control for the purpose of power allocation in massive MIMO is a well-investigated topic.

#### 3.1.1 Preliminaries

An inspection of effective SINRs in discloses qualitatively identical dependence on the power control coefficients for the four cases of uplink/downlink and zero-forcing/maximum-ratio. This permits a unified treatment of power control.

In the single-cell case, we observe that the effective SINR for terminal  $k$  can always be written in the following general form:

$$\text{SINR}_k = \frac{a_k \eta_k}{1 + \sum_{k'=1}^K b_k^{k'} \eta_{k'}}, \quad (1)$$



where  $\{a_k\}$  and  $\{b_k^{k'}\}$  are strictly positive constants, given by Table 3.1. In Table 3.1,  $M$ ,  $K$ ,  $\rho_{ul}$ ,  $\rho_{dl}$ ,  $\beta_k$ ,  $\gamma_k$  and  $\eta_k$  have the meanings as defined.

|          | Zero-Forcing  | Maximum-Ratio   |
|----------|---|---|
| Uplink   | $a_k = (M - K)\rho_{ul}\gamma_k$ $b_k^{k'} = \rho_{ul}(\beta_{k'} - \gamma_{k'})$ | $a_k = M\rho_{ul}\gamma_k$ $b_k^{k'} = \rho_{ul}\beta_{k'}$ |
| Downlink | $a_k = (M - K)\rho_{dl}\gamma_k$ $b_k^{k'} = \rho_{dl}(\beta_k - \gamma_k)$       | $a_k = M\rho_{dl}\gamma_k$ $b_k^{k'} = \rho_{dl}\beta_k$    |

**Table 3.1.** Explicit formulas for the coefficients  $\{a_k\}$  and  $\{b_k^{k'}\}$  for a single-cell system

|          | Zero-Forcing   | Maximum-Ratio   |
|----------|--|---|
| Uplink   | $a_{lk} = (M - K)\rho_{ul}\gamma_{lk}^l$ $b_{lk}^{l'k'} = \rho_{ul}(\beta_{l'k'}^l - \gamma_{l'k'}^l)$ $c_{lk}^{l'k'} = \rho_{ul}\beta_{l'k'}^l$ $d_{lk}^{l'} = (M - K)\rho_{ul}\gamma_{l'k}^l$      | $a_{lk} = M\rho_{ul}\gamma_{lk}^l$ $b_{lk}^{l'k'} = \rho_{ul}\beta_{l'k'}^l$ $c_{lk}^{l'k'} = \rho_{ul}\beta_{l'k'}^l$ $d_{lk}^{l'} = M\rho_{ul}\gamma_{l'k}^l$     |
| Downlink | $a_{lk} = (M - K)\rho_{dl}\gamma_{lk}^l$ $b_{lk}^{l'k'} = \rho_{dl}(\beta_{lk}^{l'} - \gamma_{lk}^{l'})$ $c_{lk}^{l'k'} = \rho_{dl}\beta_{lk}^{l'}$ $d_{lk}^{l'} = (M - K)\rho_{dl}\gamma_{lk}^{l'}$ | $a_{lk} = M\rho_{dl}\gamma_{lk}^l$ $b_{lk}^{l'k'} = \rho_{dl}\beta_{lk}^{l'}$ $c_{lk}^{l'k'} = \rho_{dl}\beta_{lk}^{l'}$ $d_{lk}^{l'} = M\rho_{dl}\gamma_{lk}^{l'}$ |

**Table 3.2.** Explicit formulas for the coefficients  $\{a_{lk}\}$ ,  $\{b_{lk}^{l'k'}\}$ ,  $\{c_{lk}^{l'k'}\}$  and  $\{d_{lk}^{l'}\}$  for a multi-cell system.

|          | Single-Cell  | Multi-Cell   |
|----------|--|--|
| Uplink   | $0 \leq \eta_k \leq 1$<br>$k = 1, \dots, K$  | $0 \leq \eta_{lk} \leq 1$<br>$k = 1, \dots, K, \quad l = 1, \dots, L$  |
| Downlink | $\sum_{k=1}^K \eta_k \leq 1$ <p style="text-align: center;">and</p> $\eta_k \geq 0, \quad k = 1, \dots, K$ | $\sum_{k=1}^K \eta_{lk} \leq 1, \quad l = 1, \dots, L$ <p style="text-align: center;">and</p> $\eta_{lk} \geq 0, \quad k = 1, \dots, K, \quad l = 1, \dots, L$ |

**Table 3.3.** Summary of constraints on the power control coefficients

Similarly, for the multi-cell case, from Table 4.1 the effective SINR for the  $k$ th terminal in the  $l$ th cell can be written as

$$\text{SINR}_{lk} = \frac{a_{lk}\eta_{lk}}{1 + \sum_{l' \in \mathcal{P}_l} \sum_{k'=1}^K b_{lk}^{l'k'} \eta_{l'k'} + \sum_{l' \notin \mathcal{P}_l} \sum_{k'=1}^K c_{lk}^{l'k'} \eta_{l'k'} + \sum_{l' \in \mathcal{P}_l \setminus \{l\}} d_{lk}^{l'} \eta_{l'k}} \quad (2)$$

where the non-negative coefficients  $\{a_{lk}\}$ ,  $\{b_{lk}^{l'k'}\}$ ,  $\{c_{lk}^{l'k'}\}$ , and  $\{d_{lk}^{l'}\}$  are given in Table 3.2. In Table 3.2,  $\beta_{lk}^{l'k'}$ ,  $\gamma_{lk}^{l'k'}$  and  $\eta_{lk}$  are defined. The single-cell scenario is, of course, a special case of the multi-cell scenario, obtained by setting  $\{c_{lk}^{l'k'}\}$  and  $\{d_{lk}^{l'}\}$  equal to zero and omitting the cell index  $l$ .

Table 3.3 summarizes the constraints on the power control coefficients for the single-cell and multi-cell cases. Henceforth, we denote by  $L$  the total number of cells

### 3.2 Power Control with Given SINR Targets

The problem of designing a power control policy that offers guaranteed quality-of-service can be cast as a linear feasibility problem.

### 3.2.1 Single-Cell System

We start with a single-cell system. Consider a constraint of the form

$$\text{SINR}_k \geq \overline{\text{SINR}}_k \quad k = 1, \dots, K, \quad (3)$$

Where  $\overline{\text{SINR}}_k$  is a given target *SINR* for the *k*th terminal. An *SINR* target is directly translatable to a spectral efficiency target, by using the formulas for net spectral efficiency. In practice, such a target could reflect a quality-of-service requirement for a particular terminal. The set of constraints is equivalent to the following set of inequalities:

$$a_k \eta_k \geq \overline{\text{SINR}}_k \left( 1 + \sum_{k'=1}^K b_k^{k'} \eta_{k'} \right), \quad k = 1, \dots, K, \quad (4)$$

which are linear in  $\{\eta_k\}$ . This means that the problem of designing a power control policy under which the *k*th terminal achieves an *SINR* of at least  $\overline{\text{SINR}}_k$  can be written as

$$\begin{aligned} & \text{find } \{\eta_k\} \\ & \text{subject to (i) } \text{SINR}_k \geq \overline{\text{SINR}}_k \quad k = 1, \dots, K, \quad (5) \\ & \quad \quad \quad \text{(ii) the constraints in Table 3.3} \end{aligned}$$

Problem (5) is a linear programming feasibility problem, which is easily solved using standard software toolboxes. The set of all *SINR* constraints in (3) can be satisfied for some permissible  $\{\eta_k\}$  if and only if the problem (5) has a solution.

### 3.2.2 Multi-Cell System

For the multi-cell case, we again impose a target *SINR* as a set of constraints,

$$\text{SINR}_{lk} \geq \overline{\text{SINR}}_k, \quad k = 1, \dots, K, \quad l = 1, \dots, L \quad (6)$$

where  $\text{SINR}_{lk}$  is a target SINR for the  $k$ th terminal in the  $l$ th cell. Each inequality in (6) is equivalent to the following inequality:

$$a_{lk}\eta_{lk} \geq \overline{\text{SINR}}_{lk} \left( 1 + \sum_{l' \in \mathcal{P}_1} \sum_{k'=1}^K b_{lk'}^{l'k'} \eta_{l'k'} + \sum_{l' \notin \mathcal{P}_1} \sum_{k'=1}^K c_{lk'}^{l'k'} \eta_{l'k'} + \sum_{l' \in \mathcal{P}_i \setminus \{l\}} d_{lk'}^{l'k'} \eta_{l'k'} \right) \quad (7)$$

which is linear in  $\{\eta_{lk}\}$ . Hence, a power control policy design problem of the form

$$\begin{aligned} & \text{find } \{\eta_{lk}\} \\ & \text{subject to (i) } \text{SINR}_{lk} \geq \overline{\text{SINR}}_{lk} \quad k = 1, \dots, K, \quad l = 1, \dots, L \\ & \quad \quad \quad \text{(ii) the constraints in Table 3.3} \end{aligned} \quad (8)$$

is a linear programming feasibility problem, as in the single-cell case.

### 3.3 Power allocation

The DL SE of UE  $k$  in cell  $j$  can be rewritten as

$$\text{SE}_{jk}^{\text{dl}} = \frac{\tau_d}{\tau_c} \log_2 \left( 1 + \frac{\rho_{jk} a_{jk}}{\sum_{l=1}^L \sum_{i=1}^K \rho_{li} b_{lij} + \sigma^2} \right) \quad \forall j, k \quad (9)$$

where

$$a_{jk} = |\mathbb{E}\{\mathbf{w}_{jk}^H \mathbf{h}_{jk}^j\}|^2 \quad (10)$$

and

$$b_{lij} = \begin{cases} \mathbb{E}\{|\mathbf{w}_{jk}^H \mathbf{h}_{jk}^l|^2\} & (l, i) \neq (j, k) \\ \mathbb{E}\{|\mathbf{w}_{li}^H \mathbf{h}_{jk}^l|^2\} - |\mathbb{E}\{\mathbf{w}_{li}^H \mathbf{h}_{jk}^j\}|^2 & (l, i) = (j, k) \end{cases} \quad (11)$$

are the average channel gains and average interference gains, respectively. The average is computed with respect to the small-scale fading realizations so that the DL SE is only a function of the large scale fading statistics and the choice of precoding. This is a

unique feature of Massive MIMO that largely simplifies the power allocation problem compared to single-antenna systems.

Among the different power allocation policies, two prominent examples are the max-min fairness and max product SINR strategies, which can be mathematically formalized as follows:

$$\begin{aligned}
& \max_{\{\rho_{jk}:\forall j,k\}} \min_{j,k} SE_{jk}^{\text{dl}} \\
\text{subject to} & \sum_{k=1}^K \rho_{jk} \leq P_{\max}^{\text{dl}}, \quad j = 1, \dots, L
\end{aligned} \tag{12}$$

and the max product SINR, given by

$$\begin{aligned}
& \max_{\{\rho_{jk}:\forall j,k\}} \prod_{j=1}^L \prod_{k=1}^K \gamma_{jk}^{\text{dl}} \\
\text{subject to} & \sum_{k=1}^K \rho_{jk} \leq P_{\max}^{\text{dl}}, \quad j = 1, \dots, L
\end{aligned} \tag{13}$$

where  $P_{\max}^{\text{dl}}$  denotes the maximum DL transmit power. Irrespective of the strategy, the following Monte Carlo methodology is needed to compute the optimal powers.

1) Macroscopic propagation effects

- a) Randomly drop UEs in positions  $\mathbf{x}_{\text{lr}}^j$
- b) Compute large-scale fading coefficients  $\beta_{lk}^j$
- c) Compute channel correlation matrices  $\mathbf{R}_{\text{lk}}^j$

2) Microscopic propagation effects

- a) Generate random estimated channel vectors  $\mathbf{h}_{\text{lk}}^j$  by using MMSE estimator

3) SE computation

- a) Compute precoding vectors  $\mathbf{w}_{jk}$  with MR or M-MMSE precoding
- b) Average over estimated channels to obtain  $\{a_{jk}\}$  and  $\{b_{\text{lijk}}\}$ .

4) Allocate the power by solving (12) or (13).

The solution to (12) can be obtained through a bisection approach in which a sequence of convex problems is solved, while (13) can be solved by geometric programming. Thus, both (12) and (13) require a polynomial or quasi-polynomial complexity to be solved. However, even a polynomial complexity can be too much when the solution must be obtained in real-time; that is, fast enough to be deployed in the system before the UEs positions change and the power allocation problem needs to be solved again.

## **CHAPTER 4: DIFFERENT TYPES OF POWER ALLOCATION**

### **4.1. Introduction**

The proposed power allocation algorithms are ineffective that the proposed power allocation algorithms are generally compared with basic methods such as Equal power allocation (EPA), max-min fairness power allocation, max product SINR power allocation. In this section, a comparison of these three basic power allocation algorithms with each other under the CDF state performance metric of SE per user (bit/s/Hz) is performed by considering downlink transmission for MRC, ZF and M-MMSE precoding techniques.

The different types of Power allocation techniques used are

- 1) Equal Power allocation
- 2) Maximum-Minimum fairness Power allocation
- 3) Maximum product SINR Power allocation

### **4.2 Equal Power allocation**

One of the simplest forms of power control is equal power allocation. This power control can be applied in both the uplink and the downlink transmissions. In the uplink, all the users transmit their signals with maximum available power. In the downlink, the available power is uniformly shared among all the users in the network. We note that implementing this power control is the same as having no power control in the network. This is because the eight Introduction power control coefficients do not change in response to the changes in the channel conditions in the network. As such, this rudimentary power control method does not provide a large performance boost as compared to other sophisticated power control methods. Nevertheless, equal power control is easy to implement.

Equal power allocation, in other words, Uniform power allocation is used in MIMO systems where CSI is known only at the receiver. One of the most important factors in choosing this method is that it provides low complexity. Therefore, it was

mostly preferred especially in the early days of MIMO systems. However, considering the situations where there is a limited power limit, it is important to develop different strategies. Because the same power is allocated to the user with a bad channel due to EPA, there is no effective use of power. The upper limit of the maximum capacity ratio that the communication systems can reach was determined by the study by Shannon. Therefore, the highest point where the capacities of MIMO systems can be increased is also obvious.

$$C = H(Y) - H(N) \quad (1)$$

where  $H(Y)$  and  $H(N)$  in this expression are the entropy of the received signal and the noise signal, respectively.  $\mathbf{R}_x = E \{ \mathbf{x}\mathbf{x}^H \}$ ,  $\mathbf{R}_n = E \{ \mathbf{n}\mathbf{n}^H \}$  and  $\mathbf{R}_y = E \{ \mathbf{y}\mathbf{y}^H \}$  represent the covariance matrix of transmitted signal, noise signal and received signal, respectively. In this case,  $\rho$  represents SNR.

$$\mathbf{R}_y = E [ \mathbf{y}^H \mathbf{y} ] = \rho \mathbf{H}^H \mathbf{R}_x \mathbf{H} + \mathbf{I}_{NR} \quad (2)$$

In line with this information, the capacity expression can be rewritten as

$$C = \log_2 \det ( \rho \mathbf{H}^H \mathbf{R}_x \mathbf{H} + \mathbf{I}_{NR} ) \quad (3)$$

Also, since  $\mathbf{R}_x$  is the covariance matrix of the transmitted signal, this expression can be represented as follows

$$\mathbf{R}_x = \frac{P}{N_T} \mathbf{I}_{N_T} \quad (4)$$

As a result of these equations, the capacity expression takes the form expressed in

$$C = \log_2 \det ( \mathbf{I}_{NR} + \frac{P}{N_T \sigma^2} \mathbf{H}^H \mathbf{H} ) \quad (5)$$

:



### 4.3 Maximum-Minimum fairness Power allocation

Power control is necessary to provide a uniform quality of service to all the users and promote fairness in the network. The max-min fairness Power allocation achieves fairness in the network by maximizing the minimum achievable SINR for all the users in the network. The power control problem in the multi-cell network is first formulated as a max-min optimization problem, which is then solved to find the optimal power control coefficients. When the max-min power control is applied, the SINRs for all the users in the network are equal. This max-min power control method performs well when the number of cells in the network is small. However, as the number of cells in the network increases, the power control method become less scalable. Notably, the performance of the entire network is limited by the cell experiencing the worst channel conditions. Furthermore, the achievable SINRs may approach zero when the number of cells in the network is very large.

An important design philosophy for power control policies is max-min (egalitarian) fairness, which seeks to maximize the worst SINR over all terminals. A simple proof by contradiction establishes that the max-min solution to the optimization problem provides equal SINRs for all terminals. Assume the contrary; then there is a terminal whose SINR is greater than the max-min SINR. We can reduce the power control coefficient for that terminal somewhat, which can only affect the other terminals by reducing their denominators, thereby increasing their SINRs. Consequently, the original assumption of a max-min solution is false. Max-min fairness power control therefore amounts to setting all SINR targets equal to a common value  $SINR$ , and then finding the largest possible value of SINR that ensures that all constraints in Table 3.3 are satisfied.

For a single-cell system, max-min fairness means that the SINR targets for all terminals in the cell are equal. In a multi-cell system, max-min fairness may be imposed network-wide, or independently within each cell.

A key vision of Massive MIMO is to provide uniformly good quality of service for everyone in the network. We will investigate how to optimize the pilots and powers towards this goal. We consider the pilot and data powers as optimization variables. The max-min fairness optimization problem is first formulated for the proposed pilot design as

$$\begin{aligned}
& \underset{(\hat{p}_{l,k}^b, p_{l,k} \geq 0)}{\text{maximize}} && \min_{(l,k)} \log_2 (1 + \text{SINR}_{l,k}^{\text{MR}}) \\
& \text{subject to} && \frac{1}{\tau_p} \sum_{b=1}^{\tau_p} \hat{p}_{l,k}^b \leq P_{\max,l,k}, \forall l, k, \\
& && p_{l,k} \leq P_{\max,l,k}^d, \forall l, k,
\end{aligned} \tag{1}$$

Where  $P_{\max,l,k}^d$  is the maximum power that users can provide for each data symbol. Note that this optimization problem jointly generates the pilot signals and performs power control on the pilot and data transmission. The epigraph-form representation of (1) is

$$\underset{\xi, (\hat{p}_{l,k}^b, p_{l,k} \geq 0)}{\text{maximize}} \quad \xi \tag{2}$$

$$\text{subject to} \quad \text{SINR}_{l,k}^{\text{MR}} \geq \xi, \forall l, k, \tag{3}$$

$$\frac{1}{\tau_p} \sum_{b=1}^{\tau_p} \hat{p}_{l,k}^b \leq P_{\max,l,k}, \forall l, k, \tag{4}$$

$$p_{l,k} \leq P_{\max,l,k}^d, \forall l, k. \tag{5}$$

From the expression of the SINR constraints in (3), we realize that the proposed optimization problem is a signomial program. Therefore, the max-min fairness optimization problem is NP-hard in general and seeking the optimal solution has very high complexity in any non-trivial setup. However, the power constraints (4) and (5) ensure a compact feasible domain and make the SINRs continuous functions of the optimization variables.

The optimization problem (1) requires coordination among the cells to be solved, but the main target in this paper is to investigate how much the max-min fairness SE can be improved in multi-cell Massive MIMO by joint pilot design and DL power control. One potential way to deal with practical limitations such as backhaul signalling, delays,

and scalability is to implement the optimization problem in a distributed manner using dual/primal decomposition.

The max-min fairness power allocation technique aims to maximize the worst SINR among all users. This method is used for various performance improvements in Massive MIMO systems. The basic mathematical operation of the max-min fairness power allocation method can be

$$\underbrace{\max}_{\rho_{11} \geq 0, \dots, \rho_{LK} \geq 0, \gamma \geq 0} \min \gamma \quad (6)$$

$$\frac{\rho_{jk} \alpha_{jk}}{\sum_{l=1}^L \sum_{i=1}^{K_l} \rho_{li} b_{lij} + \sigma_{UL}^2} \geq \gamma, j = 1, \dots, L, k = 1, \dots, K_j \quad (7)$$

$$\sum_{k=1}^{K_j} \rho_{jk} \leq P_{max}^{UL}, j = 1, \dots, L \quad (8)$$

As a basis, the max-min fairness power allocation algorithm can be applied to the desired performance criterion. The disadvantage of the max-min fairness power allocation algorithm is that although the algorithm focuses on improving the performance of the worst user, it creates a loss in overall network efficiency of the system.

#### 4.4 Maximum product SINR Power allocation

Max product SINR power allocation algorithm is considered in Massive MIMO systems to increase SE. Because, SE depends on a logarithmic expression of the SINR. The simplest of the power allocation methods is EPA. In addition, there is a max product SINR power allocation method that provides a balance between total SE and fairness. The aim is to maximize the SINR products of users across system.

To evaluate the performance of the power allocation, we illustrate the cumulative distribution function (CDF) of the DL SE per UE, where the randomness is due to the UE locations and shadow fading realizations. We consider ZF, MR, and M-MMSE.

The mathematical expression of the max product SINR power allocation method can be written as follows,

$$\max_{\rho_{11} \geq 0, \dots, \rho_{LK_L} \geq 0} \prod_{j=1}^L \prod_{k=1}^{K_j} \frac{\rho_{jk} \alpha_{jk}}{\sum_{l=1}^L \sum_{i=1}^{K_l} \rho_{li} b_{lij} + \sigma_{UL}^2} \quad (1)$$

$$\sum_{k=1}^{K_j} \rho_{jk} \leq P_{max}^{UL}, j = 1, \dots, L \quad (2)$$

As expected, the CDF curve with M-MMSE is to the left of the MR curve. This basically means that better performance with M-MMSE than with MR. This result might seem counterintuitive, since the M-MMSE is algorithmically and computationally more complex than MR and thus its optimal power allocation should in principle be more difficult to learn. A possible explanation for this is that with MR precoding the power is allocated only on the basis of the desired signal gain. On the other hand, with M-MMSE this is accomplished by also taking into account the power of interfering signals. Since the NN receives as input the positions of all UEs in the network, it is able to make the most of this information only when M-MMSE is employed.

To conclude, with the max-prod strategy the proposed deep learning based power allocation has significant computational complexity advantage compared to traditional approaches, while maintaining near-optimal performance with both MR and M-MMSE precoding.

#### 4.5 Deep learning based power allocation

A central goal of this work is to demonstrate that geographical location information of UEs is already sufficient as a proxy for computing the optimal powers at any given cell. This is in contrast to the traditional optimization approaches for solving (12) and (13) that require knowledge of  $\{a_{jk}\}$  and  $\{b_{lijk}\}$  in (10) and (11). We advocate using UEs' positions because they already capture the main feature of propagation channels and interference in the network. Therefore, for any given cell  $j$  the problem is to learn the *unknown* map between the solution  $\boldsymbol{\rho}_j^* = [\rho_{j1}^*, \dots, \rho_{jK}^*] \in \mathbb{R}^K$  to (12) or (13) and the  $2KL$  geographical UE positions  $\mathbf{x} = \{\mathbf{x}_{li}^i; \forall j, l, i\} \in \mathbb{R}^{2KL}$ . This is achieved by leveraging the known property of NNs that are universal function approximators. Particularly, we employ a feed forward neural network with fully-connected layers, and consisting of a  $2KL$  dimensional input layer,  $N$  hidden layers, and a  $K + 1$ -dimensional output layer yielding an estimate  $\hat{\boldsymbol{\rho}}_j = [\hat{\rho}_{j1}, \dots, \hat{\rho}_{jK}]$  of the optimal power allocation vector  $\boldsymbol{\rho}_j^*$ . Observe that the output layer has size  $K + 1$  instead of  $K$ , since we also make the NN learn  $\sum_{k=1}^K \rho_{jk}^*$  so as to satisfy the power constraint and increase the estimation accuracy.

The problem reduces to train the weights  $\mathbf{W}$  and bias terms  $\mathbf{b}$  of the NN so that the input-output map of the NN emulates the map of traditional approaches. This requires a training set containing  $N_T$  multiple samples  $\{\boldsymbol{\rho}_j^*(n), \mathbf{x}(n); n = 1, \dots, N_T\}$ , where  $\boldsymbol{\rho}_j^*(n)$  corresponds to the optimal power allocation for the training input  $\mathbf{x}(n)$ . Denoting by  $\hat{\boldsymbol{\rho}}_j(n)$  the corresponding output of the NN, the learning process consists of minimizing the following loss:

$$\min_{\mathbf{W}, \mathbf{b}} \frac{1}{N_T} \sum_{n=1}^{N_T} \ell(\hat{\boldsymbol{\rho}}_j(n), \boldsymbol{\rho}_j^*(n))$$

with  $(\cdot, \cdot)$  any suitable distance measure. Once the parameters  $\mathbf{W}$  and  $\mathbf{b}$  are configured, the NN can estimate the optimal power allocation policy also for input vectors that are not part of the training set. Therefore, every time the UEs change their positions in the

network, the power allocation can be updated by simply feeding the new positions to the NN, without having to actually solve (12) or (13).

| Parameter                                  | Value |
|--|-------|
| Number of base station antennas, $M$       | 100   |
| Number of users in each cell, $K$          | 5     |
| Number of base stations, $L$               | 4     |
| Pilot reused factor, $f$                   | 1     |
| Total transmit power per user, $\rho$ (mW) | 100   |
| Length of coherence block, $\tau_c$        | 200   |

**Table 4.1** Used parameters in massive MIMO network

#### 4.5.1 Online implementation and Complexity

The complexity of the proposed approach mainly lies in the generation of the training set. Assume that each layer is composed of  $N_i$  neurons. Computing the output of the NN requires only real multiplications and the evaluation of activation functions. Also, the training algorithm is conveniently performed by standard (stochastic) gradient descent algorithms coupled with the back-propagation algorithm. Instead, generating the training set requires to actually solve (12) or (13) for many different realizations of  $\mathbf{x}$ , by means of traditional optimization theory methods. However, this is not an issue for at least two reasons:

- The training set can be generated *off-line*. Thus, a much higher complexity can be afforded and real-time constraints do not apply.
- The training set can be updated at a much longer time-scale than the rate at which the UEs positions in the network vary. Thus, the training set can be updated at a much longer time-scale than that at which the power control

problem should be solved if traditional resource allocation approaches were used.

From the above considerations, it follows that the proposed approach grants a huge complexity reduction, which allows one to update the power allocation based on the UEs positions in real time.

## 4.6 Performance evaluation

We consider the Massive MIMO network reported in Table 4.1 with  $L = 4$  cells, with each cell covering a square area of  $250 \times 250$  m. A wrap around topology is used. We assume that  $K = 5$  UEs are randomly and uniformly distributed in each cell, at distances larger than 35 m from the BS. Results are averaged over 100 UE distributions. We consider communication over a 20 MHz bandwidth with a total receiver noise power  $\sigma^2$  of  $-94$  dBm. We assume that  $\tau_p = K$  (i.e., pilot reuse factor of 1) and that the UL transmit power  $\rho$  per UE is 20 dBm.

### 4.6.1 Maximum-product SINR

To evaluate the performance of the NN-based power allocation, we illustrate the cumulative distribution function (CDF) of the DL SE per UE, where the randomness is due to the UE locations and shadow fading realizations. We consider MR, and M-MMSE in which the NN used with both precoding schemes. The NN matches very well the optimal solution with M-MMSE. With MR precoding, a small mismatch between the two curves is observed. This basically means that the NN achieves, statistically speaking, better performance with M-MMSE than with MR. This result might seem counterintuitive, since the M-MMSE is algorithmically and computationally more complex than MR and thus its optimal power allocation should in principle be more difficult to learn. A possible explanation for this is that with MR precoding the power is allocated only on the basis of the desired signal gain. On the other hand, with M-MMSE this is accomplished by also taking into account the power of interfering signals. Since the NN receives as input the positions of all UEs in the network, it is able to make the most of this information only when M-MMSE is employed.

#### **4.6.2 Maximum-Minimum fairness**

The NNs used for the max-prod strategy, revealed to be inadequate with the max-min approach. This is probably due to the fact that the power distribution changes considerably between the two strategies. To overcome this issue, we used a different NN, which consists of two recurrent Long Short Term Memory (LSTM) layers and two dense layers. The NN matches almost exactly the theoretical curves with both MR and M-MMSE. It lacks scalability when the network size increases.



## CHAPTER 5: SIMULATION RESULTS

A comparison of the power allocation algorithms specified for SE in the downlink transmission mentioned in the previous chapter is performed. A multi-cell Massive MIMO system is considered and the parameters are given in Table 4.1. In this part where Monte Carlo simulation results are given, MR, ZF and MMSE schemes are taken into account for a multi-cell Massive MIMO system. In this system, where the number of cells is considered to be 4, each base station is located in the system center. The number of users in each cell is considered to randomly position as 10. The base station has 100 antennas.

The CDF of SE per user (bit/s/Hz) is considered as the performance metric used in the simulations. The CDF shows how SE changes depending on random user locations. Some users are in "good" locations and get high spectrum and other users are in "bad" locations and get lower spectrum. Different power allocation algorithms try to construct CDF curves in different ways. For example, the max-min equitable power allocation solution tries to make the curves nearly vertical to limit SE differences between users. Because the goal is to try to make the SE similar for users in good and bad locations.

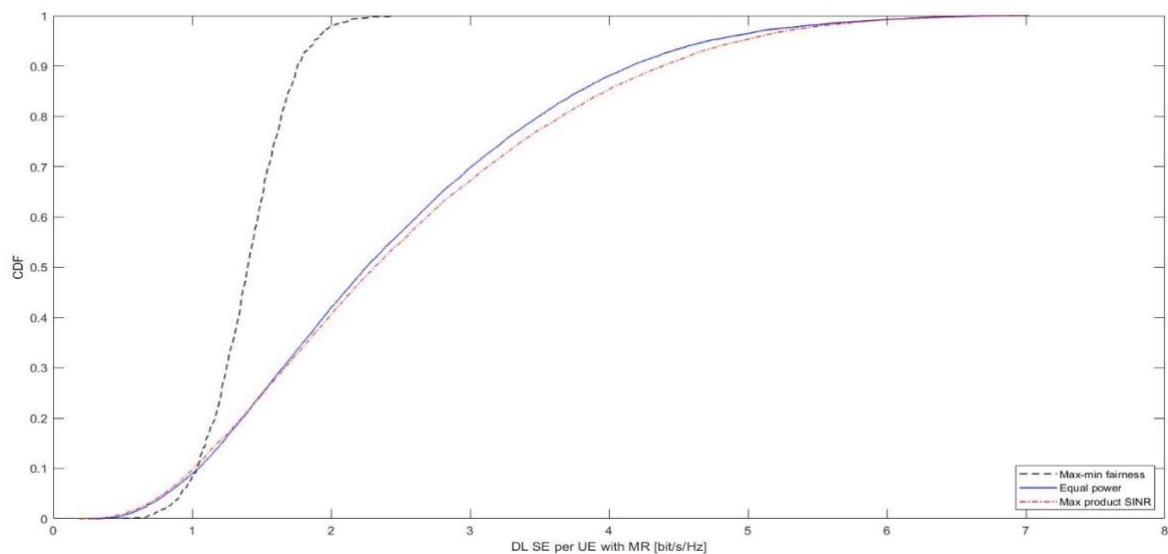


**Figure 5.1.** CDF of DL SE with MR

| Algorithm                         | CDF              | Point            |
|-----------------------------------|------------------|------------------|
|                                   | 0.9              | 0.1              |
| Max-Min Fairness power Allocation | 1.72<br>bit/s/Hz | 1.01<br>bits/Hz  |
| Equal Power Allocation            | 4.15<br>bit/s/Hz | 1.07<br>bit/s/Hz |
| Max Product SINR Power Allocation | 4.46<br>bit/s/Hz | 1.12<br>bit/s/Hz |

**Table 5.1.** SE Values for MR

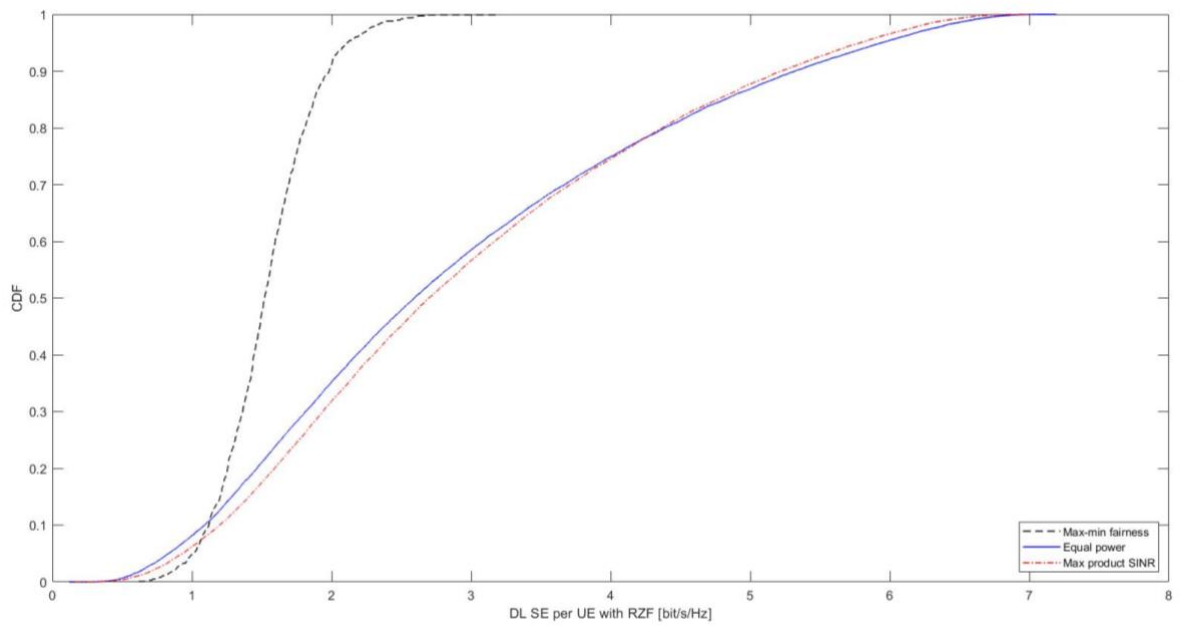


**Figure 5.2.** CDF of DL SE with ZF

| Algorithm                         | CDF Point        |                  |
|-----------------------------------|------------------|------------------|
|                                   | 0.9              | 0.1              |
| Max-Min Fairness power Allocation | 1.85<br>bit/s/Hz | 1.22<br>bit/s/Hz |
| Equal Power Allocation            | 5.27<br>bit/s/Hz | 1.13<br>bit/s/Hz |
| Max Product SINR Power Allocation | 5.34<br>bit/s/Hz | 1.43<br>bit/s/Hz |

**Table 5.2.** SE Values for ZF

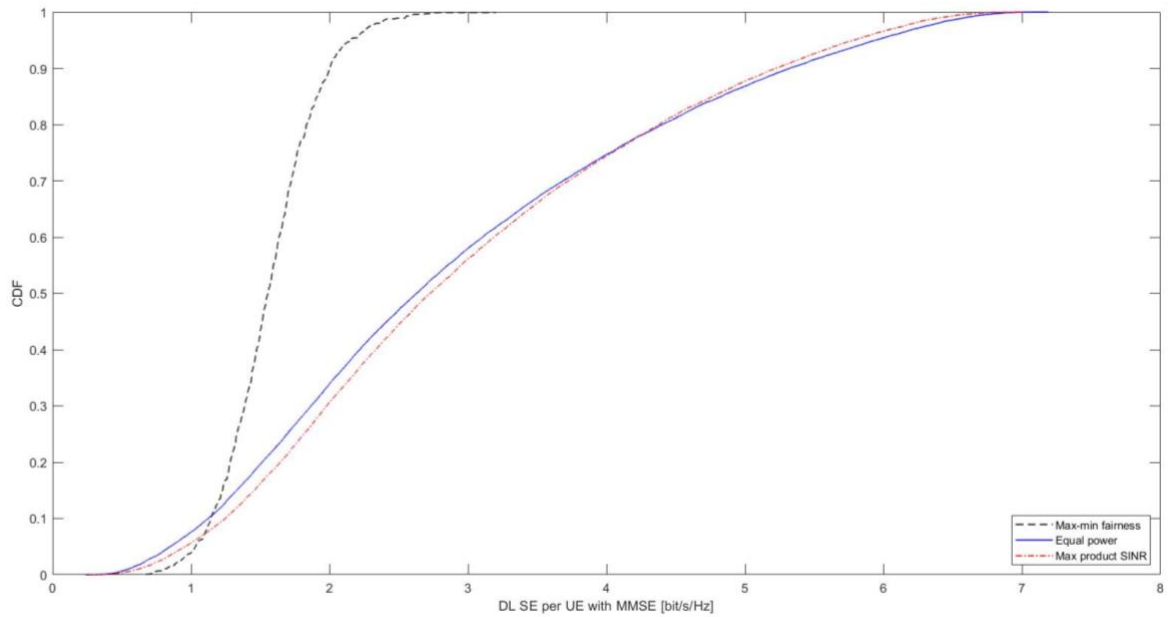


**Figure 5.3.** CDF of DL SE with MMSE

| Algorithm                         | CDF Point        |                  |
|-----------------------------------|------------------|------------------|
|                                   | 0.9              | 0.1              |
| Max-Min Fairness power Allocation | 1.94<br>bit/s/Hz | 1.36<br>bit/s/Hz |
| Equal Power Allocation            | 5.35<br>bit/s/Hz | 1.26<br>bit/s/Hz |
| Max Product SINR Power Allocation | 5.46<br>bit/s/Hz | 1.55<br>bit/s/Hz |

**Table 5.3.** SE Values for MMSE

Figure 5.1, Figure 5.2 and Figure 5.3 show the CDF of SE in a simulation with random distributions of user positions in Massive MIMO system, where the base station has 100 antennas, each cell has 5 users, and the overall number of cells is 4, according to the MR, ZF, and MMSE diagrams.

When the figures are examined, it can be seen that the best results are provided for the MMSE in total. It is also stated that this scheme is superior to MR and ZF. When comparing the remaining two schemes, MR and ZF, it is understood that ZF is more effective than MR. When the figures are examined, the results of the SE CDF at 0.9 and 0.1 for each scheme according to the power allocation algorithms are shown in Table 5.1, Table 5.2 and Table 5.3 respectively. The results for the case where all users are included in the figures.

As can be seen from the figures and tables, in the case of MRC a small percentage of users are better off with max-min fair power allocation. In the other two schemes, although the efficiency of a small percentage of users is better with EPA, max-min fair power allocation is superior to maximum power allocation of SINR products.

When interpreted in terms of power allocation algorithms, it is seen that the max-min fairness power allocation algorithm tends to users with less SE due to its working principle. Thus, it is understood that these users are trying to increase SE. This applies to all three schemes. When examined in terms of all users, it is understood that the max product SINR power allocation method gives the best results in all schemes. The EPA algorithm, on the other hand, gives a result between these two in any case. In general, it is observed that the state of the CDF curves for all three power allocation algorithms is affected by the choice of signal detection schemes to consider for the downlink.

When focusing on the graph curves, it is seen that for any scheme other than MRC, if approximately 10 percent of the users have better channels, the SE is higher with EPA. In the case of MRC, although max-min fair power allocation is ahead in this regard, it is understood that the ratios are close to each other. However, as it can be noticed from the tables, in case a small portion of users have good channels, max-min fair power allocation is at the forefront. If the random location of the users is taken into account and a certain SE value is required for the user at this location, the maximum power allocation method of SINR multiplications is a method that should be preferred.

Briefly, different results in SE of users for downlink are provided by power allocation. When evaluated in general, it has been observed that the maximum of SINR product power allocation algorithm mostly provides high SE. Which power allocation is effective for specific cases can be obtained from the results. In addition, the effect of the signal detection scheme to be used on the results is shown. Thus, the most suitable scheme can be selected.

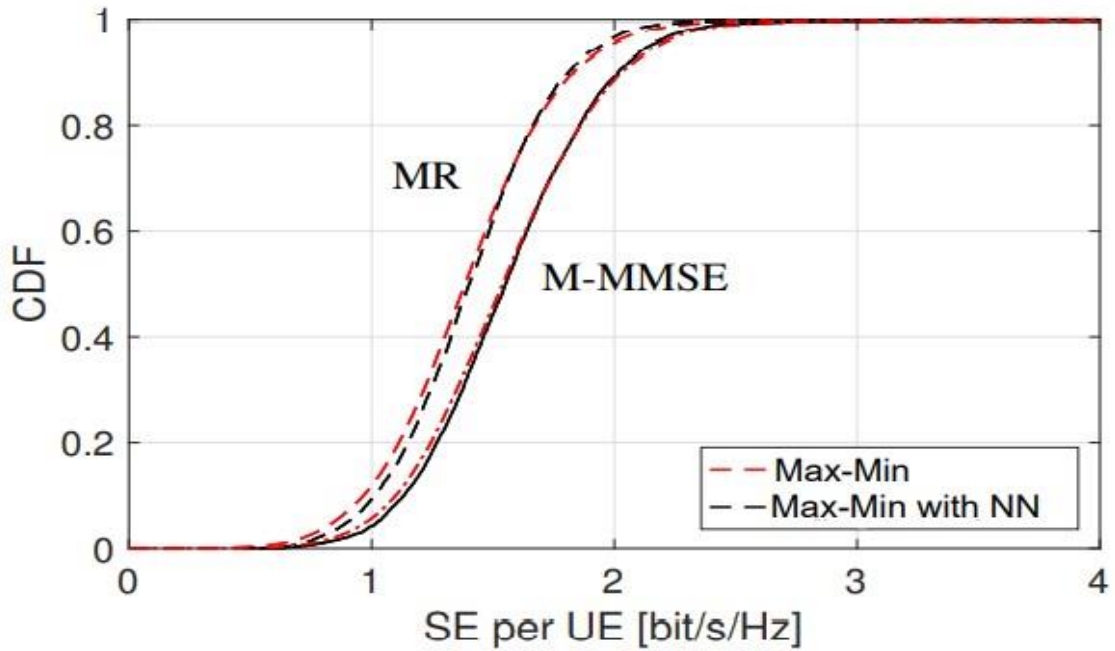


**Figure 5.4.** CDF of the DL SE per UE

| Deep Learning based<br>Power Allocation | CDF              | Point            |
|---|------------------|------------------|
|   | 0.9              | 0.1              |
| Max-Min Fairness for MR                 | 1.75<br>bit/s/Hz | 0.92<br>bit/s/Hz |
| Max-Min Fairness with NN for<br>MR      | 1.81<br>bit/s/Hz | 0.95<br>bit/s/Hz |
| Max-Min Fairness for M-MMSE             | 2.02<br>bit/s/Hz | 1.21<br>bit/s/Hz |
| Max-Min Fairness with NN for<br>M-MMSE  | 2.04<br>bit/s/Hz | 1.24<br>bit/s/Hz |

**Table 5.4.** SE Values for MR and M-MMSE

To evaluate the performance of the NN-based power allocation, we illustrate the cumulative distribution function (CDF) of the DL SE per UE, where the randomness is due to the UE locations and shadow fading realizations. We consider MR, and M-MMSE. The results of Fig.5.4 show that the NN matches very well the optimal solution

with M-MMSE. The average MSE is 0.007. With MR precoding, a small mismatch between the two curves is observed. This basically means that the NN achieves, statistically speaking, better performance with M-MMSE than with MR. This result might seem counterintuitive, since the M-MMSE is algorithmically and computationally more complex than MR and thus its optimal power allocation should in principle be more difficult to learn. A possible explanation for this is that with MR precoding the power is allocated only on the basis of the desired signal gain. On the other hand, with M-MMSE this is accomplished by also taking into account the power of interfering signals. Since the NN receives as input the positions of all UEs in the network, it is able to make the most of this information only when M-MMSE is employed.

To conclude, with the max-prod strategy the proposed deep learning based power allocation has significant computational complexity advantage compared to traditional approaches, while maintaining near-optimal performance with both MR and M-MMSE precoding.

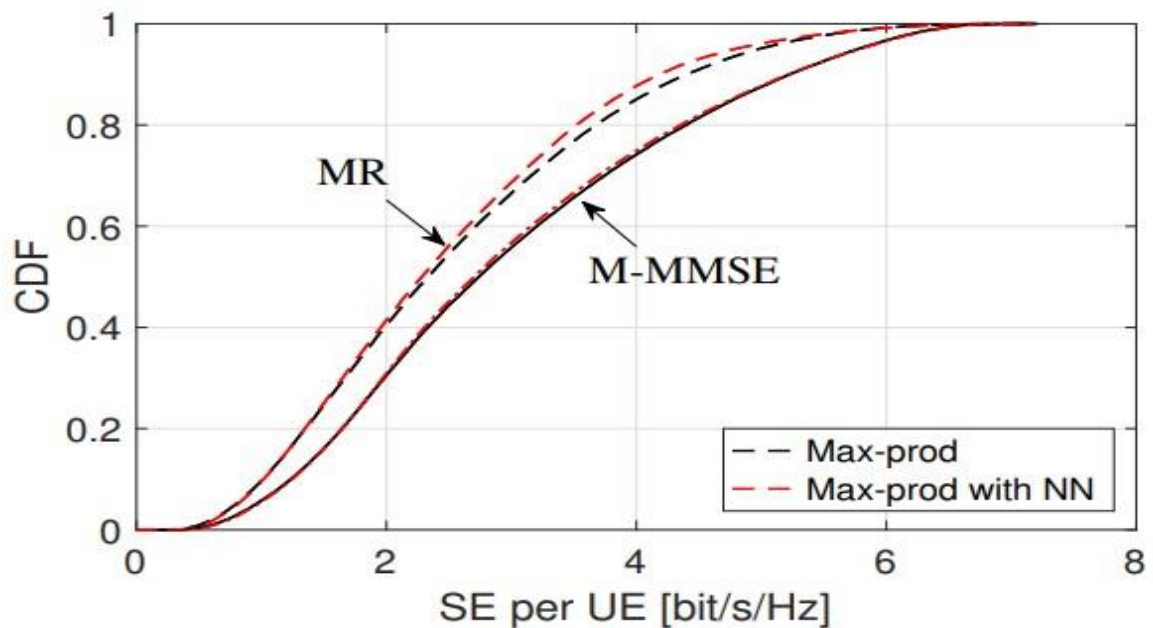


**Figure 5.5.** CDF of the DL SE per UE

| <b>Deep Learning based<br/>Power Allocation</b> | <b>CDF</b>       | <b>Point</b>     |
|---|------------------|------------------|
|   | <b>0.9</b>       | <b>0.1</b>       |
| Max Product SINR for MR                         | 4.21<br>bit/s/Hz | 1.11<br>bit/s/Hz |
| Max Product SINR with NN for<br>MR              | 4.25<br>bit/s/Hz | 1.13<br>bit/s/Hz |
| Max Product SINR for M-<br>MMSE                 | 5.52<br>bit/s/Hz | 1.22<br>bit/s/Hz |
| Max Product SINR with NN for<br>M-MMSE          | 5.53<br>bit/s/Hz | 1.24<br>bit/s/Hz |

**Table 5.5.** SE Values for MR and M-MMSE

The NNs used for the max-prod strategy, revealed to be inadequate with the max-min approach. This is probably due to the fact that the power distribution changes considerably between the two strategies. To overcome this issue, we used a different NN, which consists of two recurrent Long Short Term Memory (LSTM)<sup>1</sup> layers and two dense layers. The results of Fig.5.5 show that the NN matches almost exactly the theoretical curves with both MR and M-MMSE.



## CHAPTER 6: CONCLUSION

In this study, power allocation strategies for Massive MIMO systems are detailed. With the advancement of next-generation wireless communication technologies, it is critical to enhance spectrum and EE, in particular. For this reason, studies of power allocation algorithms, especially on spectrum and EE, have been taken into account. It is to emphasize the conditions under which power allocation algorithms proposed in these studies are performed. Massive MIMO scenarios used by detailing these conditions are also revealed. In addition, performance metrics in these studies, which focus on spectrum and EE, are specified. The techniques used in the creation of the algorithm are detailed.

After a general view of the power allocation algorithms, the power allocation strategies that are essentially covered in the literature were compared. These algorithms are EPA, max-min fairness power allocation and SINR product maximum power allocation algorithm. The examination of the SE for the multi-cell Massive MIMO system was carried out in terms of power allocation algorithms. In addition, MRC, ZF and MMSE schemes were taken into account to observe the results according to the signal detection schemes. In summary, the power allocation algorithms in Massive MIMO systems were examined especially for SE and EE.

In addition, we proposed a deep learning framework to allocate the power in the DL of a Massive MIMO network with MR and M-MMSE precoding. Two power allocation strategies were considered, namely, max-min and max-prod. We showed that with both strategies a properly trained feed-forward NN is able to learn how to allocate powers to the UEs in each cell. This is achieved by using only the knowledge of the positions of UEs in the network, thereby substantially reducing the complexity and processing time of the optimization process. Numerical results showed that the deep learning framework performs better with M-MMSE rather than with MR. This is likely due to the fact the M-MMSE allows the NN to exploit the most its available information. Moreover, the max-min policy revealed to be harder to learn.

## REFERENCES

1. E. G. Larsson, F. Tufvesson, O. Edfors, and T. L. Marzetta, “Massive MIMO for next generation wireless systems,” *IEEE Commun. Magazine*, vol. 52, no. 2, pp. 186–195, Feb. 2014.
2. Emil Björnson, Jakob Hoydis and Luca Sanguinetti (2017), “Massive MIMO Networks: Spectral, Energy, and Hardware Efficiency”, *Foundations and Trends in Signal Processing: Vol. 11, No. 3-4*, pp 154–655.
3. Emil Bjornson, Erik G. Larsson and Merouane Debbah, “Massive MIMO for Maximal Spectral Efficiency: How Many Users and Pilots Should Be Allocated?”, *IEEE Transactions on Wireless Communications*.
4. Ngo, H. Q., E. G. Larsson, and T. L. Marzetta. 2013. “Energy and spectral efficiency of very large multiuser MIMO systems”. *IEEE Trans. Commun.*61(4): 1436–1449.
5. Marzetta, T. L., E. G. Larsson, H. Yang, and H. Q. Ngo. 2016. *Fundamentals of Massive MIMO*. Cambridge University Press, 2016.
6. Q. Zhang, S.Jin, M. McKay, D. Morales Jimenez, and H.Zhu, “Power allocation schemes for multicell massive MIMO systems, ”*IEEE Trans. Wireless Commun.*, vol. 14, no. 11, pp. 5941–5955, Nov.2015.
7. H.Ngo, A.Ashikhmin, H.Yang, E.Larsson, and T.Marzetta, “Cell free massive MIMO versus small cells”, *IEEE Trans. Wireless Commun.*, vol. 16, no.3, pp. 1834–1850, Mar.2017.
8. H.Ngo, A.Ashikhmin, H.Yang, E.Larsson, and T.Marzetta, “Cell-free massive MIMO: Uniformly great service for everyone”, in *Proc. IEEE 16<sup>th</sup> Intl. Workshop on Signal Process. Advances in Wireless Commun. (SPAWC)*, Stockholm, Sweden, Jun.2015, pp. 201–205.
9. O.Saatlou, M.OmairAhmad, and M.Swamy, “Max min fairness power control for massive MUMIMO systems with finite dimensional channel model”, in *Proc. IEEE Canadian Conf. on Electrical & Computer Engineering (CCECE)*, Quebec, Canada, May2018, pp. 1–4.

10. T.Chien, E.Bjornson, and E.Larsson, "Joint power allocation and user association optimization formassive MIMO systems", *IEEE Trans. Wireless Commun.*, vol. 15, no.9, pp. 6384–6399, Sep.2016.
11. Osman Dikmen and Selmen kulac, "Power allocation algorithms for Massive MIMO Systems", *European journal of science and technology special issue* 28, pp.444-452.
12. Luca Sanguinetti, Alessio Zappone, Merouane Debbah, "Deep Learning Power Allocation in Massive MIMO", University of Pisa under the PRA 2018-2019.
13. X. Li, E. Bjornson, E. G. Larsson, S. Zhou, and J. Wang, "Massive MIMO with multi-cell MMSE processing: Exploiting all pilots for interference suppression," *EURASIP J. Wirel. Commun. Netw.*, vol. 1, no. 117, 2017.

